

MMCR: Benchmarking Cross-Source Reasoning in Scientific Papers

Yang Tian^{1*} Zheng Lu^{1,2*} Mingqi Gao^{1,3*} Zheng Liu⁴ Bo Zhao^{1†}
¹ School of AI, Shanghai Jiao Tong University ² SCUT ³ SEU ⁴ BAAI
 {yangtian6781, bo.zhao}@sjtu.edu.cn
<https://github.com/yangtian6781/MMCR>

Abstract

Fully comprehending scientific papers by machines reflects a high level of Artificial General Intelligence, requiring the ability to reason across fragmented and heterogeneous sources of information, presenting a complex and practically significant challenge. While Vision-Language Models (VLMs) have made remarkable strides in various tasks, particularly those involving reasoning with evidence source from single image or text page, their ability to use cross-source information for reasoning remains an open problem. This work presents MMCR, a high-difficulty benchmark designed to evaluate VLMs' capacity for reasoning with cross-source information from scientific papers. The benchmark comprises 276 high-quality questions, meticulously annotated by humans across 7 subjects and 10 task types. Experiments with 18 VLMs demonstrate that cross-source reasoning presents a substantial challenge for existing models. Notably, even the top-performing model, GPT-4o, achieved only 48.55% overall accuracy, with only 20% accuracy in multi-table comprehension tasks, while the second-best model, Qwen2.5-VL-72B, reached 39.86% overall accuracy. Furthermore, we investigated the impact of the Chain-of-Thought (CoT) technique on cross-source reasoning and observed a detrimental effect on small models, whereas larger models demonstrated substantially enhanced performance. These results highlight the pressing need to develop VLMs capable of effectively utilizing cross-source information for reasoning.

1. Introduction

Scientific papers encapsulate the advanced human intelligence, and it requires human experts years of study and practical experience to fully comprehend the content of these papers. Hence, comprehending scientific papers with machines is a long-standing but largely under-explored

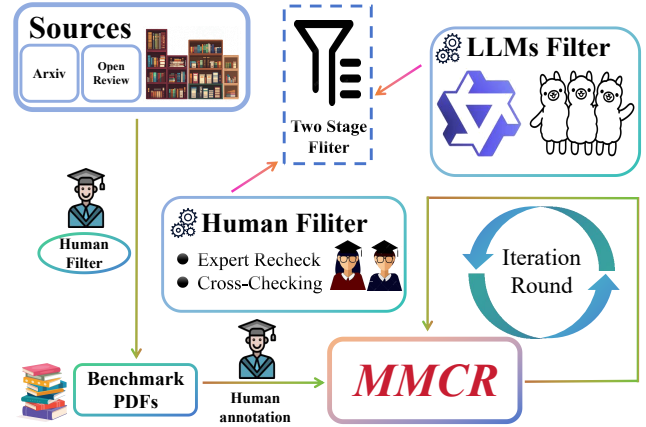


Figure 1. The construction pipeline of MMCR.

challenge. Scientific papers mainly contain elements that challenge a model's understanding and reasoning ability, such as mathematical formulas, pseudocode and figures with specialized knowledge and cross-source clues.

Recently, a variety of VLMs have emerged, including proprietary ones such as GPT-4o [12], Gemini-2.0 [28], and Claude-3 [1], as well as open-source ones such as InternVL2.5 [4], Qwen2.5-VL [3], mPLUG-DocOwl2.0 [10], LLaVA-OneVision [15], Molmo [6], CogVLM2 [9], and TextMonkey [20]. These models have demonstrated remarkable performance on general vision tasks, and many studies have explored their potential in document understanding, such as ChartQA [22], DocVQA [23], InfoVQA [24], DUDE [30], MP-DocVQA [29], etc. However, the evaluation of VLMs' capabilities in scientific paper understanding is still relatively limited.

Evaluating models for understanding scientific papers holds significant practical importance. Previous research in this domain has presented three primary limitations: 1) **Dependence on Model-Generated Annotations:** The high degree of specialization in scientific papers makes manual annotation both time-consuming and costly. For instance, ArxivQA [16] uses GPT-4v to generate Question-Answer (QA) pairs, while SCI-CQA [26] employs GPT-4o for the

*Co-first authors

†Corresponding author

Benchmarks	Avg. Pages	Cross-Page	Text	Chart	Table	Image	Pseudocode	Formula	CR	Annotation
DocVQA [23]	1.0	✗	✓	✓	✓	✓	✗	✗	✗	✓
ChartQA [22]	1.0	✗	✗	✓	✗	✗	✗	✗	✗	✗
InfoVQA [22]	1.0	✗	✗	✓	✓	✓	✗	✗	✗	✓
Charxiv [32]	1.0	✗	✗	✓	✗	✗	✗	✗	✗	✗
ArxivQA [16]	1.0	✗	✓	✓	✓	✓	✗	✗	✗	✗
MMSCI [18]	1.0	✗	✓	✓	✓	✓	✗	✗	✗	✗
DUDE [30]	5.7	✓	✓	✓	✓	✓	✗	✗	✗	✓
MP-DocVQA [29]	8.3	✗	✓	✓	✓	✓	✗	✗	✗	✗
SlideVQA [27]	20.0	✓	✓	✓	✓	✓	✗	✗	✗	✓
MMLongBench-Doc [21]	47.5	✓	✓	✓	✓	✓	✗	✗	✗	✓
MMCR	19.0	✓	✓	✓	✓	✓	✓	✓	✓	✓

Table 1. Comparison between our benchmark and previous related datasets. **Avg. Pages:** Average Pages. **Cross-Page:** Cross-Page Questions. **Text/Chart/Table/Image/Pseudocode/Formula:** Pure Text/Chart/Table/Image/Pseudocode/Formula Questions. **CR:** Cross-Source Reasoning Questions. **Annotation:** ✓: Human Annotation, ✗: Automatic Annotation, ✗: Semi-automatic Annotation.

similar task. Although these generated QA pairs are manually reviewed, they still reflect biases inherent in the generative models, which could skew the evaluation of other models. 2) **Weak Relevance of Annotations to the Article’s Content:** The specialized nature of scientific papers presents a significant challenge in dataset construction. Charxiv [32] collects papers from Arxiv but focuses solely on charts for real-world chart understanding, neglecting the specialized interpretation of these charts within the context of the articles. Similarly, MMSCI [18], which utilizes high-quality papers from *Nature Communications*, concentrates on constructing datasets around figures, without addressing the content-related questions and answers. These efforts leverage the complexity of images in scientific papers but fail to tap into the specialized knowledge embedded within the scientific paper. 3) **Lack of Cross-Source Reasoning:** In scientific papers, cross-source interactions reveal insights that are absent from a single source. The ability to integrate and reason across diverse sources is crucial, as it demonstrates a deeper and more comprehensive understanding of the paper. However, the majority of existing research [16, 26, 32] primarily focuses on understanding individual source within scientific papers. In summary, the absence of high-quality, professional benchmarks for scientific paper understanding has motivated the exploration of our work.

In this paper, we introduce MMCR, a benchmark specifically designed to evaluate the **Multi-Modality Cross-source Reasoning** capability of VLMs in scientific papers. Figure 1 outlines the annotation pipeline of our benchmark. The benchmark has been meticulously curated by expert annotators, with each paper averaging 19 pages across 7 different subjects. We have crafted 10 distinct categories of questions, totaling 276 high-quality, domain-specific questions. The benchmark has undergone filtering assisted by large language models (LLMs) and rigorous manually cross-checking, which guarantees that each question is firmly tied

to its cross-source clues and cannot be answered through alternative sources, thereby ensuring the robustness of the benchmark.

We conducted extensive experiments on MMCR to evaluate the cross-source reasoning capability of state-of-the-art VLMs in scientific papers. A total of 18 VLMs were evaluated, comprising 15 open-source models and 3 proprietary models. For each scientific paper, we re-render it into high-quality JPEG images and then are processed by the VLMs in an end-to-end approach. In other words, we expect VLMs to be able to comprehend scientific papers purely through visual input. Our results underscore the significant challenges these models face in performing cross-source reasoning of contents in scientific papers. Among the models tested, the best performer, GPT-4o, achieved an overall accuracy of only 48.55%, while the second-best model, Qwen2.5-VL-72B, reached 39.86%. Furthermore, we conducted a manual analysis of GPT-4o’s incorrect answers to identify the key bottlenecks in scientific paper understanding for current VLMs. The most frequent source of errors was perceptual error, which accounted for 27.5% of the total, revealing the perceptual defects of current models when handling multi-page scientific papers with multiple information sources. What’s more, we explored the efficacy of CoT in cross-source reasoning and found that that its performance-enhancing benefits are predominantly evident in large-scale models, which reveals the limitations of CoT in enhancing cross-source reasoning for smaller models. In summary, these findings highlight that cross-source reasoning in scientific papers remains a complex and ongoing challenge.

2. Related Work

2.1. Scientific Paper Understanding

Despite the increasing significance of automating the understanding of scientific papers, the datasets of scientific papers

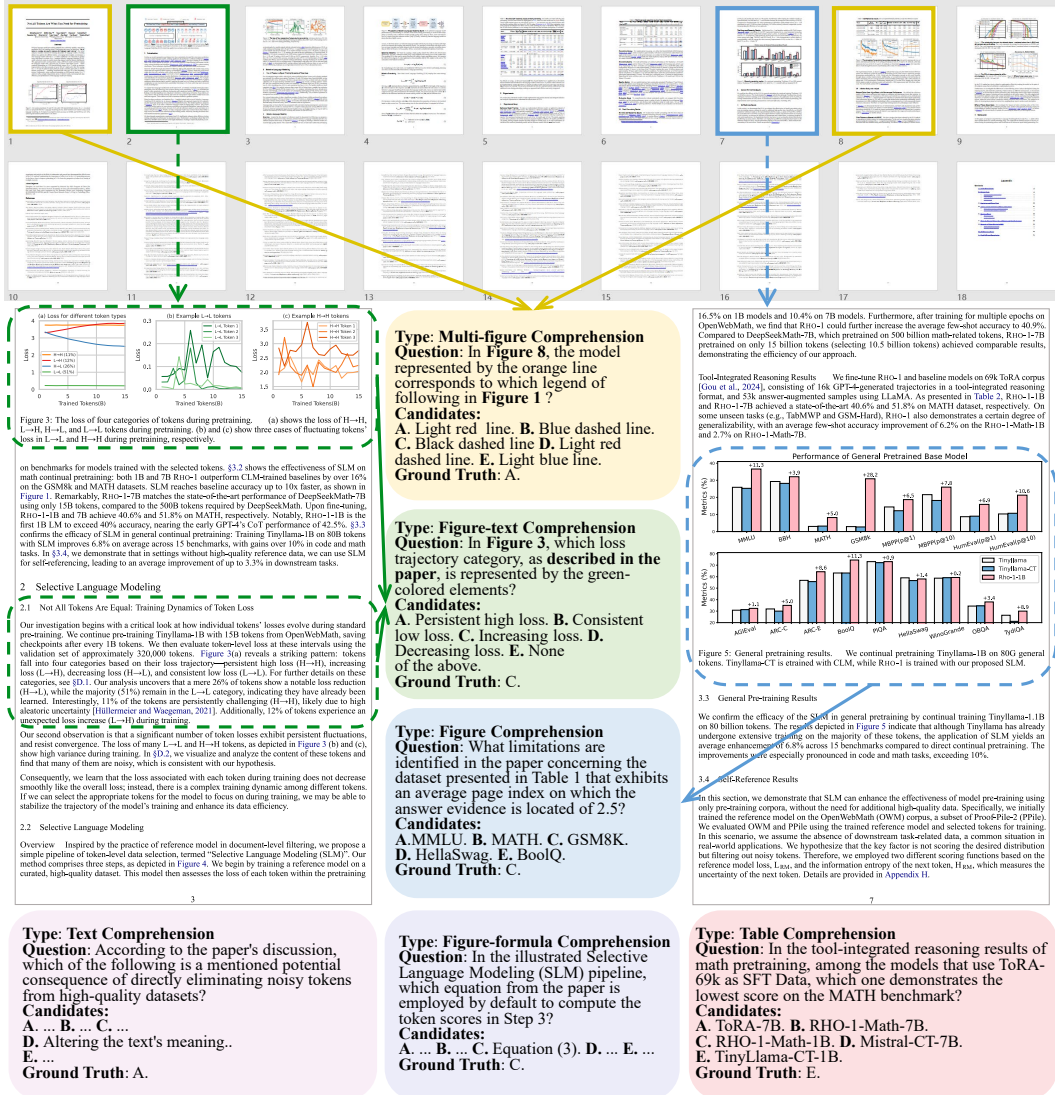


Figure 2. Examples of MMCR. We meticulously curated 10 distinct question types, each accompanied by five answer options, to assess the ability of visual-language models to perform reasoning across multiple information sources.

remain underdeveloped and insufficiently explored. In scientific paper understanding, data generation processes are mainly semi-automated. For example, Charxiv [32] collects charts from Arxiv papers and employs GPT-4v to generate QA pairs, which are then manually reviewed to ensure data quality. ArxivQA [16] also utilizes GPT-4v for generating QA pairs specific to figures in Arxiv papers. MMSCI [18], despite relying on manual annotation and selecting high-quality figures from Nature Communications, does not generate content-related QA pairs. Instead, all tasks in the MMSCI datasets are based solely on captions, with minimal connection to the actual content of the papers. Moreover, none of these datasets address cross-page understanding of the entire paper, and the information sources required for answering the questions are singular. More detailed de-

scriptions and comparisons are presented in Table 1.

2.2. Benchmarks for Document Understanding

Compared to scientific paper understanding, document understanding is more advanced in its development. While the research of document understanding has shifted focus from single-page [22–24] to multi-page understanding [13, 21, 29, 30], existing benchmarks for multi-page document understanding remain limited in critical aspects. MP-DocVQA [29], an extension of the DocVQA [23], fails to adequately assess cross-page reasoning by omitting inter-page dependency questions. Although the DUDE [30] dataset demonstrates rigorous annotation protocols with substantial manual effort, its average sample length of 5.7 pages per document provides insufficient scope for eval-

uating models on authentic multi-page challenges. Slide-VQA [27] features cross-page questioning through 20-page slides, but the inherent low information density of slides makes its task less challenging. MMLongBench-Doc [21] represents progress with comprehensive 47.5-page document samples across seven document types. However, it neglects to evaluate cross-source information synthesis, which is a crucial capability for real-world applications requiring integration of disparate information in a document. These limitations collectively highlight the need for benchmarks that simultaneously address extended document length, cross-page relationships, heterogeneous source integration, and domain-specific information density.

2.3. Models for Document Understanding

Document understanding models can be broadly categorized into two main approaches. The first relies on optical character recognition (OCR) tools, exemplified by models like LLaVA-Read [38], which use dual-stream vision encoder in conjunction with OCR tools to extract text from images, making it highly effective for text-rich image understanding tasks. The second approach is OCR-free, where models [3–5, 20, 31] process documents end-to-end without the dependency of OCR tools. Currently, there is a clear trend in document understanding models evolving from OCR-dependent architectures to OCR-free approaches.

3. MMCR Benchmark

MMCR is a comprehensive and challenging benchmark, which is designed to evaluate the cross-source reasoning capability of VLMs using multiple intertwined information sources in scientific papers. In this section, we detail the processes of data collection, question and answer annotation, quality control, and evaluation method. Finally, we present the statistical data of MMCR.

3.1. Data Collection

We collected scientific papers from both Arxiv and high-quality publications on the OpenReview platform. Due to the highly specialized nature of scientific papers, annotating them presents significant challenges for non-experts. To address this, we engaged expert annotators who are not only proficient in English reading and writing but also have extensive experience in their respective research fields. The collected papers were distributed in batches to the annotators, who were given the flexibility to select papers within their areas of expertise for annotation.

3.2. Question and Answer Annotation

Before beginning the formal annotation process, we first pre-define the annotation categories and conduct annotation exercises. These categories are based on the sources of in-

Statistic	Number
Scientific Paper	31
- Avg./Max. Pages	19 / 35
- Avg./Max. Number of Options	5 / 5
- Average Size (px)	1573 × 1210
- Maximum Size (px)	1584 × 1224
Subject	7
- 2D Object Recognition	4 (12.90%)
- Efficient AI	2 (6.45%)
- Multimodal Learning	15 (48.39%)
- Datasets and Evaluation	4 (12.90%)
- 3D from Multi-View and Sensors	1 (3.23%)
- Large Language Model	2 (6.45%)
- Robotics	3 (9.68%)
Total Questions	276
- Figure Comprehension	43 (15.58%)
- Multi-Figure Comprehension	20 (7.25%)
- Figure-Table Comprehension	26 (9.42%)
- Figure-Text Comprehension	53 (19.20%)
- Figure-Formula Comprehension	13 (4.71%)
- Table Comprehension	62 (22.46%)
- Multi-Table Comprehension	10 (3.62%)
- Text Comprehension	35 (12.68%)
- Formula Comprehension	9 (3.26%)
- Pseudocode Comprehension	5 (1.81%)

Table 2. Benchmark Statistics.

formation needed to answer the questions. Specifically, the annotation categories are as follows:

1) **Figure Comprehension:** Figures in scientific papers serve as visual representations of models, theories, data, and other key elements. Questions based on these figures assess the model’s ability to interpret and understand the visual information they convey. What’s more, the annotated questions do not specify which figure is being referenced, thereby evaluating the model’s ability to comprehend figures in the context of a multi-page scientific paper.

2) **Multi-Figure Comprehension:** In scientific papers, figures are often not standalone elements but are interconnected with other figures. By reasoning across multiple figures, it avoids being limited to the interpretation of individual figures, leading to more comprehensive conclusions. These questions evaluate the model’s ability to utilize information across figures to answer effectively. Through meticulous verification, we ensure that all the necessary evidence for reasoning is confined to the relevant set of figures, with no information sourced from elsewhere.

3) **Figure-Table Comprehension:** The figure provides rich graphical information, while the table offers detailed structured data. These questions require VLMs to grasp the underlying relationships between graphical and structured information and perform reasoning across both sources.

Model	Date	#Param	Overall	FIC	MF	FTA	FTE	FF	TAC	MT	TEC	FOC	PC
<i>Open-Source Multimodal Large Language Models</i>													
<i>4-9B Models</i>													
Phi-3.5-Vision [2]	2024-09	4B	4.71	6.98	5.00	0.00	5.66	0.00	3.23	0.00	11.43	0.00	0.00
YI-VL [36]*	2024-06	6B	4.35	2.33	15.00	3.85	5.66	7.69	1.61	0.00	5.71	0.00	0.00
Molmo-7B-O [6]*	2024-09	7B	0.36	0.00	0.00	0.38	0.00	0.00	0.00	0.00	0.00	0.00	0.00
XComposer2.5 [37]*	2024-07	7B	3.99	4.65	20.00	0.00	3.77	0.00	3.22	0.00	2.86	0.00	0.00
mPLUG-Owl3 [35]	2024-07	7B	7.61	18.60	20.00	3.85	3.77	7.69	4.84	0.00	5.71	0.00	0.00
Qwen2.5-VL [3]	2025-01	7B	21.74	16.28	25.00	7.69	26.42	30.77	16.13	10.00	45.71	11.11	0.00
Bunny [8]*	2024-06	8B	4.71	4.65	10.00	3.85	1.89	0.00	4.84	0.00	5.71	11.11	20.00
Idefics3 [14]	2024-08	8B	9.78	11.63	10.00	7.69	7.55	15.38	6.45	10.00	20.00	0.00	0.00
MiniCPM-o 2.6 [11]	2025-01	8B	10.51	13.53	5.00	11.54	5.66	0.00	6.45	0.00	31.43	0.00	20.00
InternVL2.5 [4]	2024-12	8B	12.32	11.63	15.00	7.69	13.21	7.69	4.84	0.00	31.43	22.22	0.00
GLM-4v [7]*	2024-06	9B	2.54	2.33	5.00	0.00	5.66	0.00	1.61	0.00	0.00	11.11	0.00
<i>11-78B Models</i>													
Llama3.2-Vision [25]*	2024-09	11B	1.81	0.00	0.00	0.00	0.00	7.69	3.23	0.00	5.71	0.00	0.00
DeepSeek-VL2 [33]	2024-05	27B	1.09	0.00	0.00	0.00	5.66	0.00	0.00	0.00	0.00	0.00	0.00
InternVL2.5 [4]	2024-12	78B	14.49	18.60	20.00	7.69	11.32	7.69	6.45	0.00	34.29	22.22	20.00
Qwen2.5-VL [3]	2025-01	72B	<u>39.86</u>	<u>30.23</u>	<u>35.00</u>	26.92	<u>50.94</u>	38.46	<u>35.48</u>	0.00	68.57	33.33	<u>40.00</u>
<i>Proprietary Multimodal Large Language Models</i>													
GPT-4o mini [12]	2024-07	-	32.61	25.58	<u>35.00</u>	26.92	39.62	<u>46.15</u>	30.65	10.00	37.14	33.33	40.00
GeminiFlash2.0 [28]	2024-12	-	34.42	23.26	30.00	<u>30.77</u>	39.62	30.77	<u>35.48</u>	30.00	40.00	<u>44.44</u>	60.00
GPT-4o [12]	2024-11	-	48.55	44.19	40.00	46.15	54.72	84.61	37.10	<u>20.00</u>	<u>65.71</u>	55.56	<u>40.00</u>

Table 3. Evaluation of various models on MMCR. We evaluate model performance across ten categories of scientific comprehension tasks: Figure Comprehension (FIC), Multi-figure Comprehension (MF), Figure-Table Comprehension (FTA), Figure-Text Comprehension (FTE), Figure-Formula Comprehension (FF), Table Comprehension (TAC), Multi-table Comprehension (MT), Text Comprehension (TEC), Formula Comprehension (FOC), Pseudocode Comprehension (PC). For each category, we report both individual accuracy rates and overall performance metrics. The best results are marked **bold** and the second results are underlined. * indicate that the input images are concatenated into one image.

4) **Figure-Text Comprehension:** Figures in scientific papers enormously necessitate specialized contextual knowledge for full comprehension. Questions of this task evaluate a model’s ability to integrate information from both figures and text content to formulate accurate answers. If the model lacks a deep understanding of the text or fails to interpret the figures properly, these questions can pose considerable challenges.

5) **Figure-Formula Comprehension:** Formulas provide essential supplementary details that are crucial for understanding the content of figures. These questions evaluate a model’s ability to answer queries that require interpreting both figures and formulas. To generate accurate responses, the model must effectively integrate the relevant formula with the corresponding figure.

6) **Table Comprehension:** Tables in scientific papers serve as a foundational component for empirical analysis. These questions are designed to evaluate the model’s ability to extract information from individual tables and reason without explicitly referencing a specific table in the queries. This approach assesses the model’s capacity to interpret and navigate tables within a scientific paper.

7) **Multi-table Comprehension:** Scientific papers frequently include multiple tables, and drawing conclusions through cross-table comparisons is a common practice. This task assesses a model’s capability to extract and integrate information from several tables, enabling it to synthesize insights from diverse data sources effectively.

8) **Text Comprehension:** Given that scientific papers are text-dense, these questions evaluate a model’s ability to extract and understand meaningful information from scientific papers.

9) **Formula Comprehension:** Formulas present condensed, symbolic information, which poses a greater challenge for the model compared to plain text. This task tests the model’s ability to understand and extract information from the formulas in scientific papers.

10) **Pseudocode Comprehension:** Although pseudocode appears less frequently than figures or tables in scientific papers, it often provides crucial additional context. These questions test the model’s ability to interpret the symbolic and graphical components of pseudocode.

Figure 2 presents an annotated example. The questions are designed to assess the model’s ability not only to derive

answers from cross-source information but also to comprehend content across pages, as relevant evidence may be distributed throughout the document. This presents heightened challenges for the model’s performance. Detailed examples are provided in the supplementary material.

In our answer annotation process, we employed a multiple-choice format that required annotators to generate a minimum of eight questions per scientific paper. To ensure diversity in question types, annotators were instructed to avoid repetitive question patterns. Each question was mandated to have five distinct answer options; questions that could not meet this requirement were excluded. Papers yielding fewer than eight valid questions were omitted from the annotation.

3.3. Quality Control

To enhance the annotation quality of the benchmark, we implemented a two-round semi-automatic quality control procedure that combines the merits of manual annotations and LLMs.

LLMs-Assisted Data Filtering. Despite the meticulous efforts of our annotators, some questions addressed general knowledge that large language models could accurately answer based solely on their internal knowledge or by reasoning directly from the question and options. To evaluate this, we employed two language models, Llama-3.3-70B [25] and Qwen2.5-72B [34], to perform reasoning using only the questions and options as input, without incorporating any associated scientific papers, images, or supplementary text. Questions that the models answered correctly were flagged as potential low-quality questions. However, before discarding these questions entirely, we carefully reviewed the reasoning processes of the models to ensure their correct answers were not the result of random guessing.

Cross-Checking. Annotators conducted parallel cross-checking of each other’s work to enhance the quality of the benchmark. Errors identified during this process were either corrected or eliminated. Furthermore, a voting mechanism was implemented to filter out question-and-answer pairs that were overly similar in structure or content, ensuring greater diversity and reliability in the final benchmark.

3.4. Evaluation Method

With only five answer options, randomly selecting an option would result in an accuracy of approximately 20%, which potentially reduces the discernible performance differences among VLMs. To address this, and inspired by MMBench [19], we implemented a circular evaluation to further minimize the likelihood of the model guessing the correct answer. In this approach, the order of the answer options is rotated five times and presented to the VLMs. A model is considered to have successfully solved the problem only if it answers correctly in all five tests.

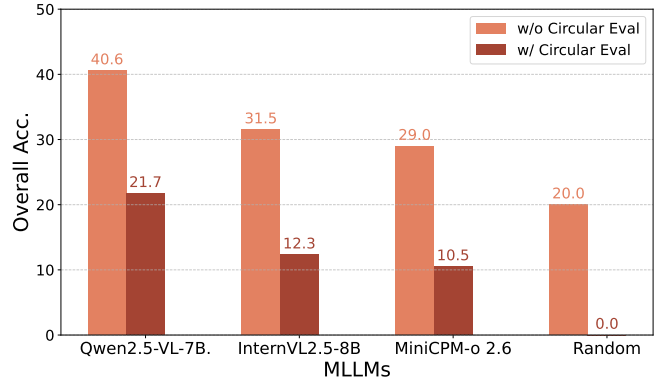


Figure 3. Comparison of the overall accuracy of VLMs with and without circular eval.

3.5. Statistics of Benchmark

The detailed statistics of our benchmark are presented in Table 2. This benchmark is distinguished by its focus on cross-source reasoning, encompassing a total of 31 scientific papers with an average length of 19 pages per paper, spanning 7 diverse subjects. A total of 276 questions have been annotated, distributed across 10 distinct categories, with an average of 8.9 questions per paper. This comprehensive benchmark is designed to rigorously evaluate the capability of VLMs to perform reasoning by integrating information from multiple sources within scientific papers.

4. Experiments and Analysis

4.1. Evaluation Protocol

We conduct a three-step evaluation protocol: response generation, answer extraction, and score calculation. Specifically, in the answer generation stage, we deliberately refrain from imposing task-specific constraints on the model, allowing it to generate responses freely. Subsequently, we apply a heuristic rule-based extraction method to extract the model’s output. The specific heuristic rule-based extraction method is described in detail in the supplementary material. Finally, we compute the exact match score to evaluate the model’s performance. We report both the overall accuracy as well as the accuracy for each individual category.

4.2. Experimental Setup

We evaluated 18 VLMs, comprising 15 open-source models and 3 proprietary models. To rigorously assess the models’ capability for reasoning across multiple sources of information in scientific papers, we re-rendered the PDF-format papers into high-resolution JPEG images at 144 DPI and fed them into the VLMs in an end-to-end approach. However, not all models support multi-image input. For those not trained on multi-image or video datasets, we concatenated the high-resolution JPEG images into a single large

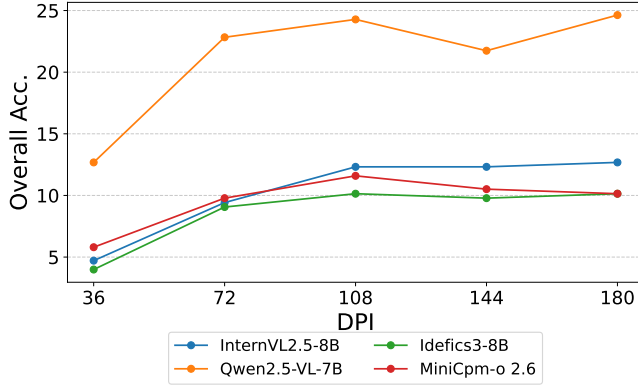


Figure 4. Model performance on increasing rendering DPI.

image before inputting it into the models. For models that do support multi-image input, we conducted evaluations using the native multi-image input method.

4.3. Main Results

The experimental results are comprehensively summarized in Table 3, which details both category-specific and overall accuracy metrics. From these findings, three principal conclusions emerge:

Proprietary models demonstrate superior performance. The proprietary GPT-4o model achieved state-of-the-art results on our benchmark, attaining overall accuracy of 48.55%. This represents an 8.69% performance advantage over the leading open-source model, Qwen2.5-VL-72B. Notably, GPT-4o matched or exceeded Qwen2.5-VL-72B’s performance across nine distinct question categories, underscoring the persistent performance gap in multi-modal reasoning capabilities between proprietary and open-source architectures for scientific document analysis.

Current VLMs face significant challenges in reasoning with cross-source information. Even the highest-performing proprietary VLM (GPT-4o) failed to surpass 50% overall accuracy, while demonstrating sub-50% performance in five question categories. Open-source models exhibited more pronounced limitations, with most models achieving less than 10% overall accuracy. These results collectively highlight the inherent challenge of our benchmark.

Tabular comprehension presents unique difficulties. Comparative analysis revealed that 72.22% (13/18) of evaluated models exhibited equal or inferior performance on table comprehension questions compared to figure comprehension questions. When extended to multi-element comprehension tasks, all tested models demonstrated equivalent or reduced accuracy. This systematic performance discrepancy suggests inherent challenges in tabular data interpretation within complex scientific papers.

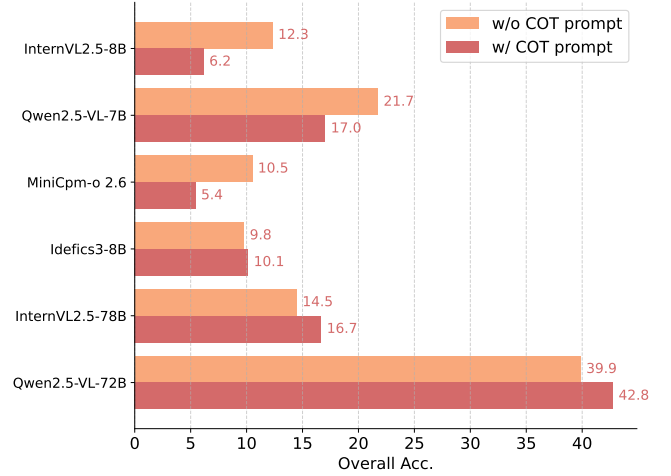


Figure 5. Comparison of the overall accuracy of VLMs with and without CoT prompt.

4.4. Is Circular Evaluation more Robust?

In Figure 3, we evaluated three models and theoretical random selection with and without circular evaluation. As shown in the figure, all three models experienced significant performance degradation under circular evaluation, with MiniCPM-o 2.6’s performance dropping to approximately 36% of its performance without circular evaluation. The accuracy of random selection decreased from 20% to $0.2^5 \times 100\%$. These results demonstrate that circular evaluation substantially reduces the probability of obtaining correct answers through random selection, validating the robustness of our benchmark.

4.5. Does High-Resolution Image Input Improve Model Performance?

In the case of single-image input, increasing the image resolution typically enhances model performance [5, 15, 17],. However, with multi-page image input, the large number of visual tokens present a significant challenge for the model in extracting useful information. Further increasing the image resolution also increases the number of visual tokens. How do the rich information and large number of visual tokens brought by high-resolution images affect the model’s performance? To explore this question, we conducted experiments using four VLMs. The DPI of PDF-rendered JPEG images was gradually increased from 36 to 180. As shown in Figure 4, all four models exhibited steady performance improvements as the DPI increased to 108. However, when DPI exceeds 108, the model’s performance fluctuates and even declines as DPI increases. This suggests that while moderately increasing resolution can benefit model performance for multi-image inputs, the model struggles to handle images with excessively high resolution.

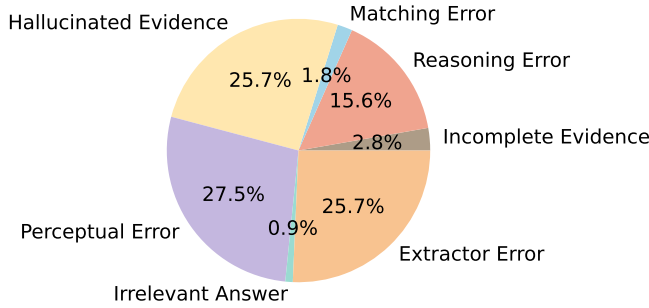


Figure 6. Error distribution over 109 annotated GPT-4o errors.

4.6. Does CoT Help in Answering Cross-Source Reasoning Questions?

Figure 5 presents the impact of CoT prompt on our benchmark. Specifically, we designed CoT prompt, as outlined in the supplementary material, and evaluated the performance of the VLMs with and without CoT prompt. Our experiments revealed that smaller models experienced a notable performance decline when using CoT prompt. To explore this further, we evaluated larger models, such as InternVL2.5-78B and Qwen2.5-VL-72B, and observed that their performance improved with the use of CoT prompt. We hypothesize that the smaller models may struggle with severe hallucinations when confronted with a high number of visual tokens, or they may fail to identify sufficient sources of evidence in tasks requiring cross-source reasoning, which leads to a significant drop in CoT performance. In contrast, the larger models appear better equipped to handle the complexity of visual tokens and more effectively retrieve relevant evidence for coherent chain-of-thought reasoning. Interestingly, for the Idefics3-8B model, CoT prompt led to a slight improvement in performance. A detailed review of the Idefics3-8B reasoning process revealed that it still delivered answers directly without engaging in reasoning under the CoT prompt. These results highlight the varying effects of CoT across models of different sizes, particularly in their capacity to leverage cross-source information in multi-page scientific papers. They suggest that the ability to effectively extract and integrate cross-source information from numerous visual tokens is key to improving performance with CoT prompt.

4.7. Error Analysis

We further conducted an error analysis to identify the bottlenecks in current multimodal models when handling cross-source reasoning tasks. Specifically, we selected 109 instances where GPT-4o provided incorrect answers and performed a manual examination. The errors were categorized into the following types: 1) **Hallucinated Evidence**: The model failed to locate the necessary evidence to answer the question. 2) **Incomplete Evidence**: The evidence retrieved

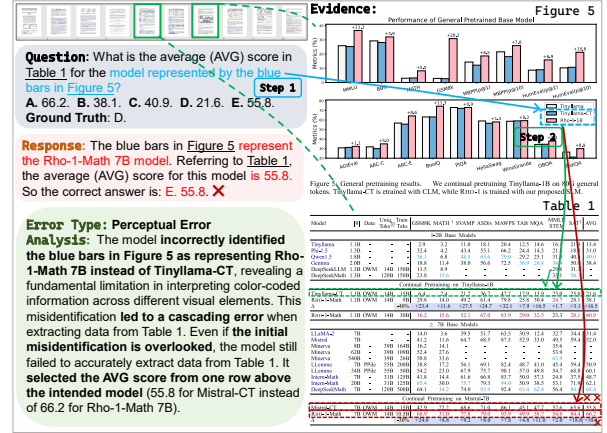


Figure 7. An example of a perceptual error is observed in GPT-4o, where the model fails to accurately interpret both the figure and the table, resulting in unsuccessful cross-source reasoning. The correct reasoning process is outlined in Step 1 and Step 2.

was insufficient. 3) **Perceptual Error**: The model misinterpreted graphs, symbols, colors, etc. 4) **Extractor Error**: The model extracted values that did not exist in the table or extracted values from misaligned tables. 5) **Reasoning Error**: The model made incorrect inferences based on the retrieved information. 6) **Irrelevant Answer**: The model’s answer was unrelated to the question. 7) **Matching Error**. Rule-based methods failed to extract the correct response from the model. The distribution of these errors is shown in Figure 6. Our findings reveal that the most prevalent error is perceptual error, followed by extractor error, highlighting the model’s difficulty in accurately retrieving relevant information from multi-page images. Hallucinated and incomplete evidence together account for 28.5% of the errors, further underscoring the substantial room for improvement in current VLMs in leveraging cross-source information for reasoning. Figure 7 presents our analysis of a perceptual error, offering insights into its underlying causes.

5. Conclusion

In this work, we present MMCR, a benchmark for evaluating VLMs’ ability to perform cross-source reasoning in scientific papers. Our extensive experiments reveal that current VLMs struggle to identify complete and accurate evidence required for reasoning from cross-source information in scientific papers. We hope that the development of this benchmark will promote advancement in VLMs’ capabilities to perform reasoning utilizing cross-source information.

Acknowledgement. This work was funded by National Natural Science Foundation of China under No. 62306046. We thank MolarData for their technical and resource support.

References

- [1] The claude 3 model family: Opus, sonnet, haiku. 1
- [2] Marah Abdin, Jyoti Aneja, Hany Awadalla, Ahmed Awadallah, Ammar Ahmad Awan, Nguyen Bach, Amit Bahree, Arash Bakhtiari, Jianmin Bao, Harkirat Behl, et al. Phi-3 technical report: A highly capable language model locally on your phone. *arXiv preprint arXiv:2404.14219*, 2024. 5
- [3] Shuai Bai, Keqin Chen, Xuejing Liu, Jialin Wang, Wenbin Ge, Sibao Song, Kai Dang, Peng Wang, Shijie Wang, Jun Tang, et al. Qwen2. 5-vl technical report. *arXiv preprint arXiv:2502.13923*, 2025. 1, 4, 5
- [4] Zhe Chen, Weiyun Wang, Yue Cao, Yangzhou Liu, Zhangwei Gao, Erfei Cui, Jinguo Zhu, Shenglong Ye, Hao Tian, Zhaoyang Liu, et al. Expanding performance boundaries of open-source multimodal models with model, data, and test-time scaling. *arXiv preprint arXiv:2412.05271*, 2024. 1, 5
- [5] Zhe Chen, Weiyun Wang, Hao Tian, Shenglong Ye, Zhangwei Gao, Erfei Cui, Wenwen Tong, Kongzhi Hu, Jiapeng Luo, Zheng Ma, et al. How far are we to gpt-4v? closing the gap to commercial multimodal models with open-source suites. *Science China Information Sciences*, 67(12):220101, 2024. 4, 7
- [6] Matt Deitke, Christopher Clark, Sangho Lee, Rohun Tripathi, Yue Yang, Jae Sung Park, Mohammadreza Salehi, Niklas Muennighoff, Kyle Lo, Luca Soldaini, et al. Molmo and pixmo: Open weights and open data for state-of-the-art multimodal models. *arXiv preprint arXiv:2409.17146*, 2024. 1, 5
- [7] Team GLM, Aohan Zeng, Bin Xu, Bowen Wang, Chenhui Zhang, Da Yin, Diego Rojas, Guanyu Feng, Hanlin Zhao, Hanyu Lai, Hao Yu, Hongning Wang, Jiadai Sun, Jiajie Zhang, Jiale Cheng, Jiayi Gui, Jie Tang, Jing Zhang, Juanzi Li, Lei Zhao, Lindong Wu, Lucen Zhong, Mingdao Liu, Minlie Huang, Peng Zhang, Qinkai Zheng, Rui Lu, Shuaiqi Duan, Shudan Zhang, Shulin Cao, Shuxun Yang, Weng Lam Tam, Wenyi Zhao, Xiao Liu, Xiao Xia, Xiaohan Zhang, Xiaotao Gu, Xin Lv, Xinghan Liu, Xinyi Liu, Xinyue Yang, Xixuan Song, Xunkai Zhang, Yifan An, Yifan Xu, Yilin Niu, Yuantao Yang, Yueyan Li, Yushi Bai, Yuxiao Dong, Zehan Qi, Zhaoyu Wang, Zhen Yang, Zhengxiao Du, Zhenyu Hou, and Zihan Wang. Chatglm: A family of large language models from glm-130b to glm-4 all tools, 2024. 5
- [8] Muyang He, Yexin Liu, Boya Wu, Jianhao Yuan, Yueze Wang, Tiejun Huang, and Bo Zhao. Efficient multimodal learning from data-centric perspective. *arXiv preprint arXiv:2402.11530*, 2024. 5
- [9] Wenyi Hong, Wei Han Wang, Ming Ding, Wenmeng Yu, Qingsong Lv, Yan Wang, Yean Cheng, Shiyu Huang, Junhui Ji, Zhao Xue, et al. Cogvlm2: Visual language models for image and video understanding. *arXiv preprint arXiv:2408.16500*, 2024. 1
- [10] Anwen Hu, Haiyang Xu, Liang Zhang, Jiabo Ye, Ming Yan, Ji Zhang, Qin Jin, Fei Huang, and Jingren Zhou. mplug-docowl2: High-resolution compressing for ocr-free multi-page document understanding. *arXiv preprint arXiv:2409.03420*, 2024. 1
- [11] Shengding Hu, Yuge Tu, Xu Han, Chaoqun He, Ganqu Cui, Xiang Long, Zhi Zheng, Yewei Fang, Yuxiang Huang, Weilin Zhao, et al. Minicpm: Unveiling the potential of small language models with scalable training strategies. *arXiv preprint arXiv:2404.06395*, 2024. 5
- [12] Aaron Hurst, Adam Lerer, Adam P Goucher, Adam Perelman, Aditya Ramesh, Aidan Clark, AJ Ostrow, Akila Welihinda, Alan Hayes, Alec Radford, et al. Gpt-4o system card. *arXiv preprint arXiv:2410.21276*, 2024. 1, 5
- [13] Pranab Islam, Anand Kannappan, Douwe Kiela, Rebecca Qian, Nino Scherrer, and Bertie Vidgen. Financebench: A new benchmark for financial question answering. *arXiv preprint arXiv:2311.11944*, 2023. 3
- [14] Hugo Laurençon, Andrés Marafioti, Victor Sanh, and Léo Tronchon. Building and better understanding vision-language models: insights and future directions. In *Workshop on Responsibly Building the Next Generation of Multimodal Foundational Models*, 2024. 5
- [15] Bo Li, Yuanhan Zhang, Dong Guo, Renrui Zhang, Feng Li, Hao Zhang, Kaichen Zhang, Peiyuan Zhang, Yanwei Li, Ziwei Liu, et al. Llava-onevision: Easy visual task transfer. *arXiv preprint arXiv:2408.03326*, 2024. 1, 7
- [16] Lei Li, Yuqi Wang, Runxin Xu, Peiyi Wang, Xichong Feng, Lingpeng Kong, and Qi Liu. Multimodal arxiv: A dataset for improving scientific comprehension of large vision-language models. *arXiv preprint arXiv:2403.00231*, 2024. 1, 2, 3
- [17] Zhang Li, Biao Yang, Qiang Liu, Zhiyin Ma, Shuo Zhang, Jingxu Yang, Yabo Sun, Yuliang Liu, and Xiang Bai. Monkey: Image resolution and text label are important things for large multi-modal models. In *Proceedings of the IEEE/CVF Conference on Computer Vision and Pattern Recognition*, pages 26763–26773, 2024. 7
- [18] Zekun Li, Xianjun Yang, Kyuri Choi, Wanrong Zhu, Ryan Hsieh, HyeonJung Kim, Jin Hyuk Lim, Sungyoung Ji, Byungju Lee, Xifeng Yan, et al. Mmsci: A dataset for graduate-level multi-discipline multimodal scientific understanding. *arXiv preprint arXiv:2407.04903*, 2024. 2, 3
- [19] Yuan Liu, Haodong Duan, Yuanhan Zhang, Bo Li, Songyang Zhang, Wangbo Zhao, Yike Yuan, Jiaqi Wang, Conghui He, Ziwei Liu, et al. Mmbench: Is your multi-modal model an all-around player?(2023). *arXiv preprint arXiv:2307.06281*, 2023. 6
- [20] Yuliang Liu, Biao Yang, Qiang Liu, Zhang Li, Zhiyin Ma, Shuo Zhang, and Xiang Bai. Textmonkey: An ocr-free large multimodal model for understanding document. *arXiv preprint arXiv:2403.04473*, 2024. 1, 4
- [21] Yubo Ma, Yuhang Zang, Liangyu Chen, Meiqi Chen, Yizhu Jiao, Xinze Li, Xinyuan Lu, Ziyu Liu, Yan Ma, Xiaoyi Dong, et al. Mmlongbench-doc: Benchmarking long-context document understanding with visualizations. *arXiv preprint arXiv:2407.01523*, 2024. 2, 3, 4
- [22] Ahmed Masry, Do Xuan Long, Jia Qing Tan, Shafiq Joty, and Enamul Hoque. Chartqa: A benchmark for question answering about charts with visual and logical reasoning. *arXiv preprint arXiv:2203.10244*, 2022. 1, 2, 3
- [23] Minesh Mathew, Dimosthenis Karatzas, and CV Jawahar. Docvqa: A dataset for vqa on document images. In *Proceed-*

- ings of the *IEEE/CVF winter conference on applications of computer vision*, pages 2200–2209, 2021. [1](#), [2](#), [3](#)
- [24] Minesh Mathew, Viraj Bagal, Rubèn Tito, Dimosthenis Karatzas, Ernest Valveny, and CV Jawahar. Infographicvqa. In *Proceedings of the IEEE/CVF Winter Conference on Applications of Computer Vision*, pages 1697–1706, 2022. [1](#), [3](#)
- [25] AI Meta. Llama 3.2: Revolutionizing edge ai and vision with open, customizable models. *Meta AI Blog*. Retrieved December, 20:2024, 2024. [5](#), [6](#)
- [26] Lingdong Shen, Kun Ding, Gaofeng Meng, Shiming Xiang, et al. Rethinking comprehensive benchmark for chart understanding: A perspective from scientific literature. *arXiv preprint arXiv:2412.12150*, 2024. [1](#), [2](#)
- [27] Ryota Tanaka, Kyosuke Nishida, Kosuke Nishida, Taku Hasegawa, Itsumi Saito, and Kuniko Saito. Slidevqa: A dataset for document visual question answering on multiple images. In *Proceedings of the AAAI Conference on Artificial Intelligence*, pages 13636–13645, 2023. [2](#), [4](#)
- [28] Gemini Team, Rohan Anil, Sebastian Borgeaud, Jean-Baptiste Alayrac, Jiahui Yu, Radu Soricut, Johan Schalkwyk, Andrew M Dai, Anja Hauth, Katie Millican, et al. Gemini: a family of highly capable multimodal models. *arXiv preprint arXiv:2312.11805*, 2023. [1](#), [5](#)
- [29] Rubèn Tito, Dimosthenis Karatzas, and Ernest Valveny. Hierarchical multimodal transformers for multipage docvqa. *Pattern Recognition*, 144:109834, 2023. [1](#), [2](#), [3](#)
- [30] Jordy Van Landeghem, Rubèn Tito, Łukasz Borchmann, Michał Pietruszka, Paweł Joziak, Rafał Powalski, Dawid Jurkiewicz, Mickaël Coustaty, Bertrand Anckaert, Ernest Valveny, et al. Document understanding dataset and evaluation (dude). In *Proceedings of the IEEE/CVF International Conference on Computer Vision*, pages 19528–19540, 2023. [1](#), [2](#), [3](#)
- [31] Peng Wang, Shuai Bai, Sinan Tan, Shijie Wang, Zhihao Fan, Jinze Bai, Keqin Chen, Xuejing Liu, Jialin Wang, Wenbin Ge, et al. Qwen2-vl: Enhancing vision-language model’s perception of the world at any resolution. *arXiv preprint arXiv:2409.12191*, 2024. [4](#)
- [32] Zirui Wang, Mengzhou Xia, Luxi He, Howard Chen, Yitao Liu, Richard Zhu, Kaiqu Liang, Xindi Wu, Haotian Liu, Sadhika Malladi, et al. Charxiv: Charting gaps in realistic chart understanding in multimodal llms. *arXiv preprint arXiv:2406.18521*, 2024. [2](#), [3](#)
- [33] Zhiyu Wu, Xiaokang Chen, Zizheng Pan, Xingchao Liu, Wen Liu, Damai Dai, Huazuo Gao, Yiyang Ma, Chengyue Wu, Bingxuan Wang, et al. Deepseek-vl2: Mixture-of-experts vision-language models for advanced multimodal understanding. *arXiv preprint arXiv:2412.10302*, 2024. [5](#)
- [34] An Yang, Baosong Yang, Beichen Zhang, Binyuan Hui, Bo Zheng, Bowen Yu, Chengyuan Li, Dayiheng Liu, Fei Huang, Haoran Wei, et al. Qwen2. 5 technical report. *arXiv preprint arXiv:2412.15115*, 2024. [6](#)
- [35] Jiabo Ye, Haiyang Xu, Haowei Liu, Anwen Hu, Ming Yan, Qi Qian, Ji Zhang, Fei Huang, and Jingren Zhou. mplug-owl3: Towards long image-sequence understanding in multi-modal large language models. *arXiv preprint arXiv:2408.04840*, 2024. [5](#)
- [36] Alex Young, Bei Chen, Chao Li, Chengen Huang, Ge Zhang, Guanwei Zhang, Guoyin Wang, Heng Li, Jiangcheng Zhu, Jianqun Chen, et al. Yi: Open foundation models by 01. ai. *arXiv preprint arXiv:2403.04652*, 2024. [5](#)
- [37] Pan Zhang, Xiaoyi Dong, Yuhang Zang, Yuhang Cao, Rui Qian, Lin Chen, Qipeng Guo, Haodong Duan, Bin Wang, Linke Ouyang, et al. Internlm-xcomposer-2.5: A versatile large vision language model supporting long-contextual input and output. *arXiv preprint arXiv:2407.03320*, 2024. [5](#)
- [38] Ruiyi Zhang, Yufan Zhou, Jian Chen, Jiuxiang Gu, Changyou Chen, and Tong Sun. Llava-read: Enhancing reading ability of multimodal language models. *arXiv preprint arXiv:2407.19185*, 2024. [4](#)

Appendix

A. Benchmark Details

We appreciate the reviewer’s thoughtful comment on MMCR’s classification as a reasoning benchmark. We respectfully maintain that MMCR tests reasoning capabilities as it aligns with the reviewer’s cited definition of reasoning as “multi-step/multi-hop question answering.” Our definition of “cross-source reasoning” in MMCR refers to questions that require synthesizing information from multiple sources within scientific papers to derive answers that cannot be obtained from any single source alone.

Taking the question in Figure S.7 as an example, the reasoning process in MMCR directly parallels HotpotQA’s definition of “inferring the bridge entity to complete the 2nd-hop question.” As illustrated in Figure S.7, answering MMCR questions typically requires first inferring which specific figure or table is being referenced through textual descriptions (e.g., “the t-SNE visualization of CLIP encoding features”). This constitutes the first reasoning hop and establishes the critical bridge entity. Only after successfully identifying this bridge entity can the model proceed to the second hop, extracting relevant information from the identified sources and synthesizing it to derive the answer.

The reasoning complexity is further amplified by scientific papers’ high information density (19 pages average), input as pure images rather than OCR-processed text, and questions requiring numerical reasoning and calculations. The benchmark comprises scientific papers across seven academic subjects of artificial intelligence, with questions systematically categorized into ten distinct types based on their required evidence sources. The distribution of these categories is illustrated in Fig. S.8. Representative examples demonstrating each evidence type are presented in Figs. S.12 to S.21.

B. Evaluation Details

B.1. Evaluation Prompt

Figure S.9 presents the prompts with and without the use of Chain-of-Thought (CoT). For InternVL2.5, we employed the official CoT prompt released by the developers. For the remaining benchmark models—MiniCpm-o 2.6, Qwen2.5-VL, and Idefics3—we implemented a unified CoT prompt to ensure methodological consistency across experiments.

B.2. Answer Option Inference Details for LLM Responses

B.2.1. Implementation Details

Unlike existing benchmarks that employ LLM-based methods for open-ended response extraction, our benchmark utilizes a heuristic rule-based approach for multiple-choice answer inference.

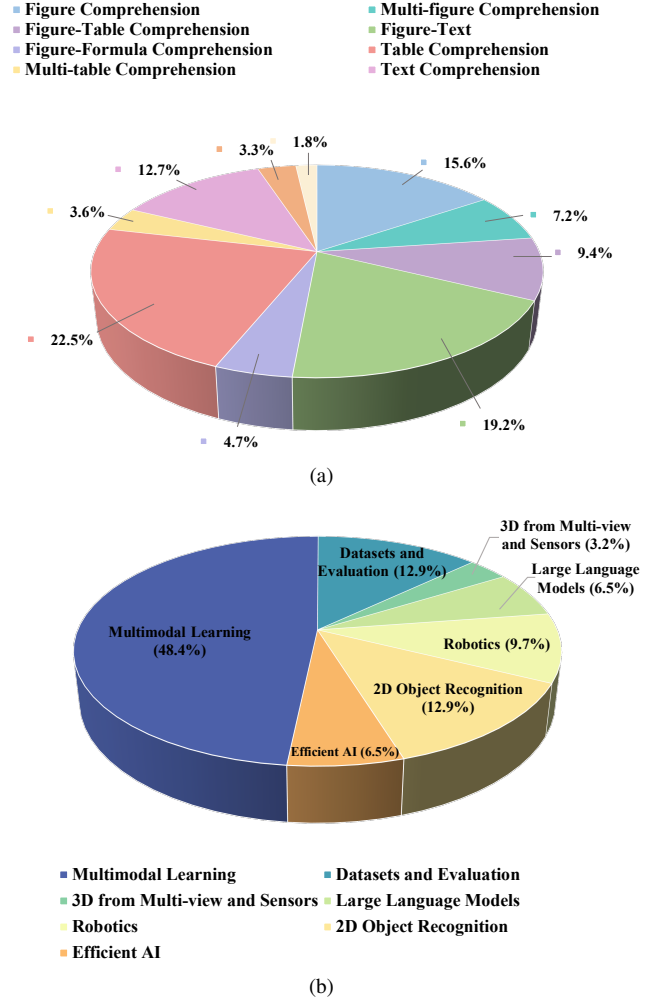


Figure S.8. Distribution of Questions by Evidence Types and Research Domains. (a) Percentage distribution across ten evidence source types. (b) Distribution across seven AI research subjects.

The rule-based approach for multiple-choice answer inference comprises two stages: primary option-based inference, followed by text-based inference as a fallback strategy. Specifically, the option-based inference method counts the occurrence of option identifiers (A, B, C, etc.) in the response. A valid inference is made when exactly one option identifier is detected. When option-based inference fails, the text-based inference serves as a fallback mechanism. It converts both the model response and choice contents to lowercase before searching for exact matches of choice content within the response. This method succeeds only when precisely one choice content is found in the processed response.

This two-stage approach ensures robust answer extraction while maintaining high precision through strict matching criteria. When both methods fail to identify a unique answer, false will be returned to indicate inference failure.

Evaluation Prompts: CoT Prompt

CoT Prompt for InternVL-2.5:

“Your task is to answer the question below. Give step by step reasoning before you answer, and when you’re ready to answer, please use the format:

‘\Final answer: ... \’

Question: {question}”

CoT Prompt for MiniCpm-o 2.6, Qwen2.5-VL, Idedfics3:

“Carefully read the following multichoice question, solve it step by step and finally pick the option associated with the correct answer in the format of ‘Answer: Selected option.’”

w/o CoT Prompt:

“Please select the correct answer from the options above.”

Figure S.9. Evaluation Prompt

B.2.2. Existing Problems

The rule-based approach for multiple-choice answer inference offers efficiency by eliminating additional LLM calls. However, it occasionally fails to accurately extract responses despite correct model reasoning. We categorize such cases as *Matching Errors*. As shown in Tab. S.4. The error distribution analysis demonstrates that extraction failures represent a negligible proportion of the total errors, with only two instances identified across all cases. Figure S.28 illustrates one representative example of such a Matching Error.

Matching errors	Total error cases	Error Rate
2	109	1.8%

Table S.4. Example Distribution of Matching Errors in Response Extraction from GPT-4o. The table shows the proportion of matching errors among all error cases, demonstrating that extraction failures constitute only 1.8% of total errors identified in our evaluation.

C. Extended Analysis

C.1. Analysis of Error Cases

We conducted systematic error analysis of GPT-4o’s performance on our benchmark to investigate its limitations in cross-source reasoning within scientific papers. Through manual examination of 109 incorrect responses, we identified seven distinct error categories. A comprehensive analysis of all error categories, accompanied by representative examples, is presented in (Figs. S.22 to S.28).

C.2. Performance Across Evidence Types

We analyze model performance across different evidence source types, with detailed results presented in Fig. S.10. The radar chart visualization demonstrates GPT-4o’s consistent superiority across most categories compared to the other five VLMs. Particularly in text comprehension tasks, both QwenVL-2.5-72B and GPT-4o achieve notable accuracy (68.57 and 65.71 respectively), likely benefiting from their extensive pretraining corpora.

However, substantial performance degradation is observed in cross-source integration tasks featured in MMCR, particularly in Figure-Text Comprehension, Figure-Table Comprehension, and Multi-Figure Comprehension, where the majority of VLMs achieve accuracy scores below 50. The pronounced disparity between single-source and cross-source task performance reveals a fundamental limitation: while MLLMs exhibit proficiency in individual modality processing, they demonstrate reduced effectiveness in tasks requiring synthesis of information from heterogeneous sources.

C.3. Annotation requirements

Before initiating the formal annotation process, a systematic taxonomy of task types and subject domains was established. This methodological framework ensures annotation consistency and maintains rigorous quality standards across the dataset construction process. Rigorous quality control protocols were implemented throughout the annotation process to establish a robust benchmark for evaluating the comprehensive capabilities of VLMs. Question formulation followed a structured protocol that integrates document-specific content with domain knowledge requirements, establishing a rigorous framework for in-depth assessment of scientific paper comprehension. The questions in MMCR are designed to evaluate comprehensive document understanding, specifically focusing on cross-source reasoning capabilities. The detailed evaluation requirements are illustrated in Fig. S.11.

C.4. Annotation process

The annotation process was conducted by expert annotators, who underwent comprehensive training to ensure annotation consistency and quality standards. The standardized training protocol comprised several systematic phases: 1) **Initial standardization:** The project leader provided annotated sample papers to the annotators, which were subject to multiple rounds of verification. This iterative process ensured that the annotators fully understood the expectations and standards required for the annotation. 2) **Domain-specific allocation:** Annotators were assigned to subject domains aligned with their primary research expertise, selecting one to two domains from predefined categories. Within each domain, five representative publica-

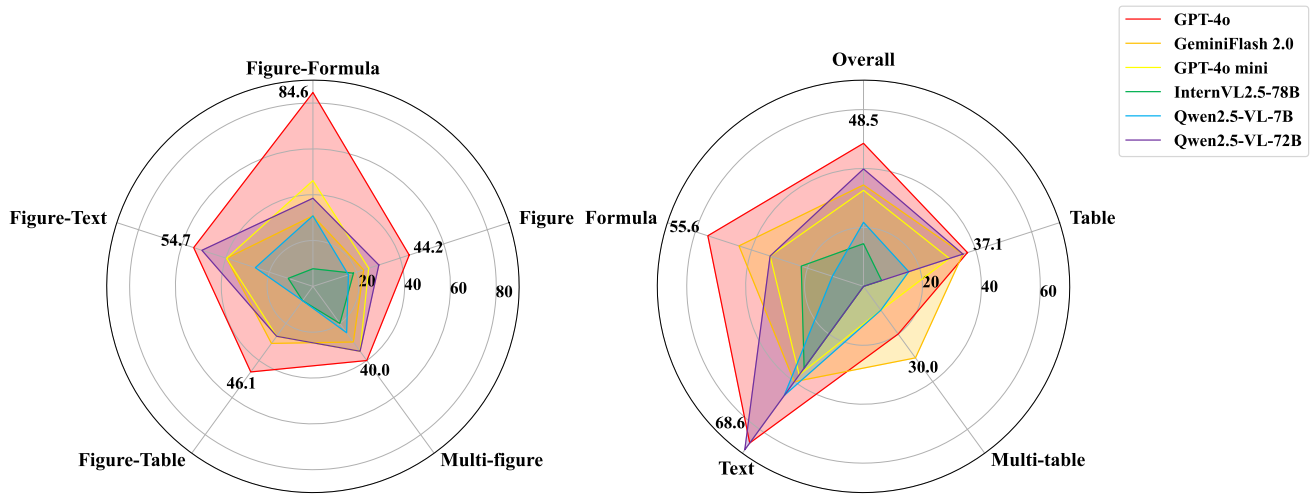


Figure S.10. Fine-grained results on various evidence source types.

tions were systematically identified for annotation. This domain-specific allocation ensures optimal alignment between expert knowledge and content analysis, maintaining annotation quality and disciplinary rigor. 3) **Quality assurance:** Completed annotations underwent systematic review by the project coordinator to ensure adherence to established protocols. When deviations from annotation standards were identified, annotators received structured feedback and supplementary training for remediation. This iterative quality assurance process continued until all annotations achieved compliance with predetermined quality benchmarks. 4) **Supplementary annotation:** In the final phase, expert annotators conducted supplementary annotation rounds in accordance with established protocols to expand the dataset while maintaining consistency standards.

Examples for Annotation Requirements

Requirement I:

“The question is specifically designed to examine the cross-source reasoning ability of the model in scientific papers, and it must be correctly derived exclusively from the designated information source, not from any additional information source. Annotators must strictly adhere to this requirement.”

Requirement II:

“In order to mitigate the risk of the model relying exclusively on prior knowledge to generate responses, the annotated questions and answers were meticulously structured to ensure that accurate responses could only be derived by synthesizing information distributed across multiple pages of the document. This approach prevents the model from bypassing the intended reasoning process and reduces the potential for information leakage or unintended biases that might arise from relying on external knowledge.”

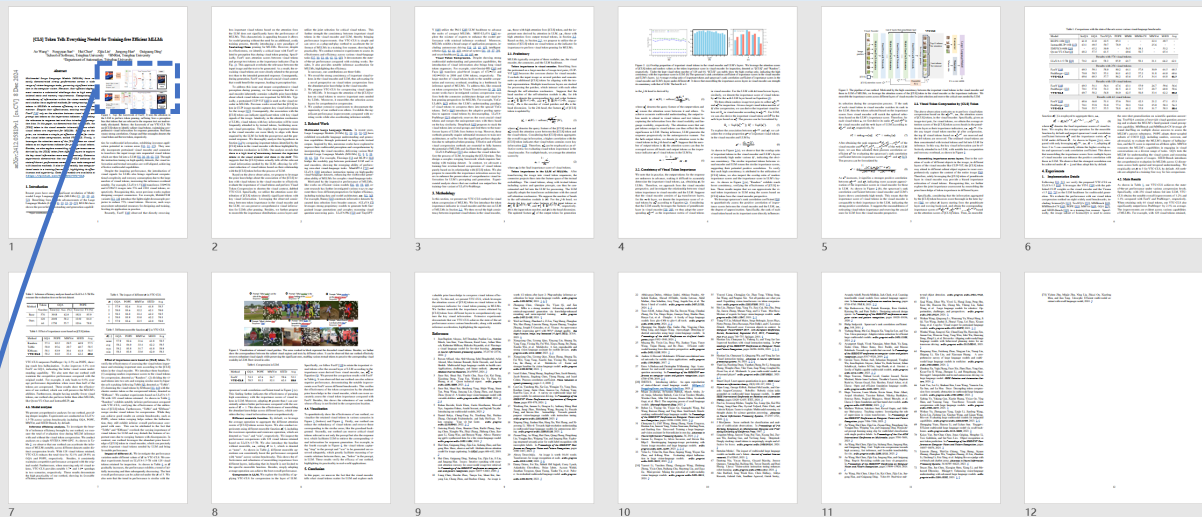
Requirement III:

“To further ensure that the model genuinely comprehends the content of each paper, at least eight questions were annotated for every paper. This requirement was set to ensure a robust and comprehensive evaluation of the model’s understanding across a variety of aspects within each paper.”

Figure S.11. Annotation requirements

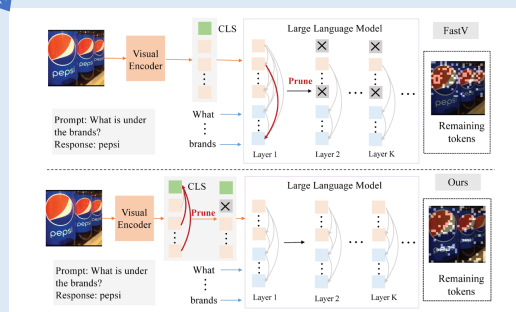
Figure Comprehension

Document Thumbnail



Question: In the comparative illustration of the FastV and VTC-CLS frameworks, what specific colors are used to represent vision tokens and text tokens, respectively?

Evidence:



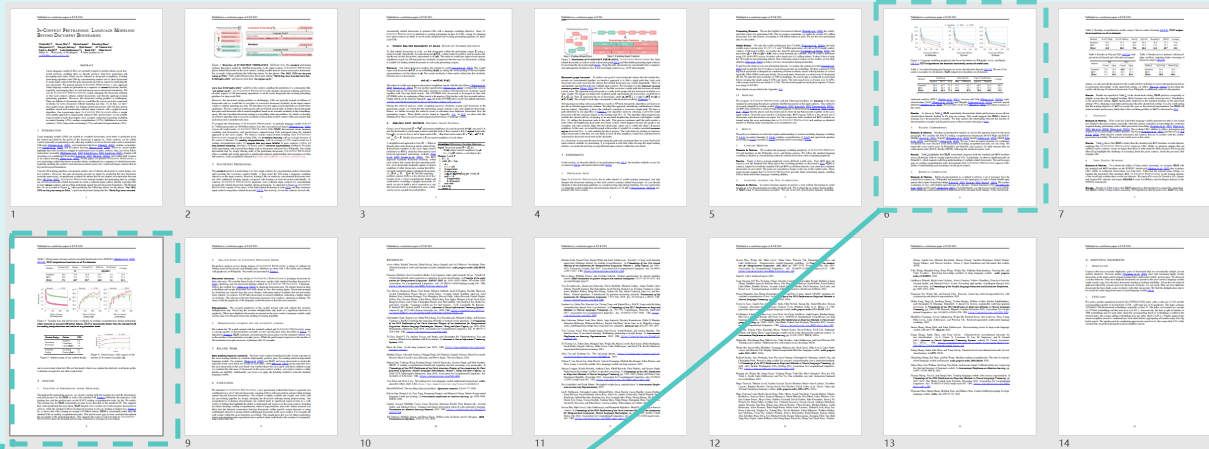
- A. Green and light orange.
- B. Light orange and light blue.
- C. Green and light blue.
- D. Gray and light blue.
- E. Light blue and light orange.

Ground Truth: B. Light orange and light blue.

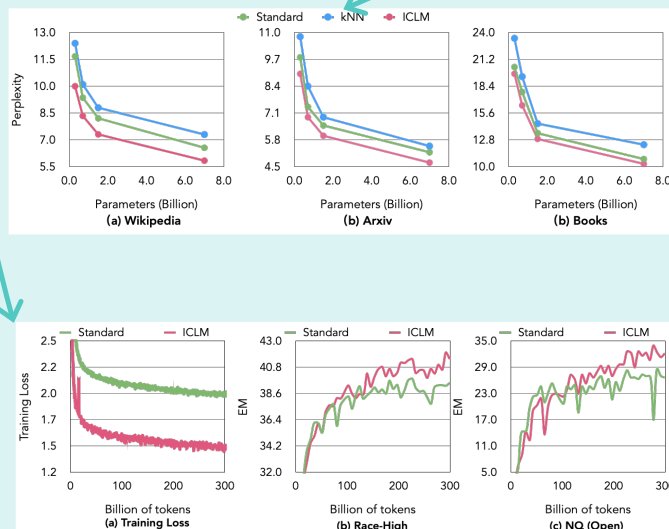
Figure S.12. The demo of figure comprehension.

Multi-figure Comprehension

Document Thumbnail:



Evidence:



Question: Which of the following methods is consistently represented in both the language modeling perplexity charts across multiple datasets and the training loss and performance evolution graphs for reading comprehension during pretraining?

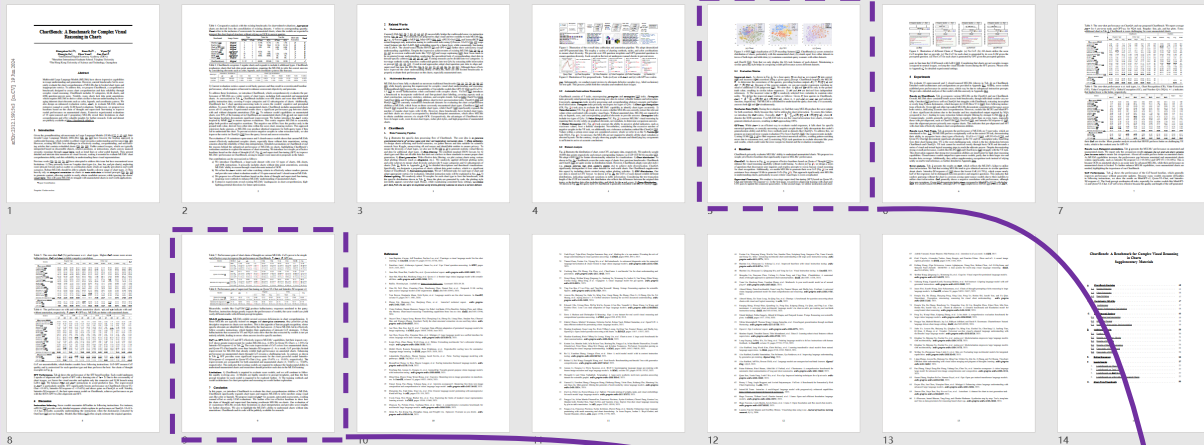
- A. Standard and kNN.
- B. ICLM and Standard.
- C. ICLM and kNN.
- D. Standard, kNN and ICLM.
- E. Only ICLM.

Ground Truth: B. ICLM and Standard.

Figure S.13. The demo of multi-figure comprehension.

Figure-Table Comprehension

Document Thumbnail:



Question: In the t-SNE visualization of CLIP encoding features for Chart type data, what color represents the dataset that achieves the highest average score(75.76) among open-source MLLMs in the zero-shot performance comparison table?

Evidence:

Models	ChartBench						ChartQA				
	Regular Type			Extra Type			Avg	Rank	Human	Avg	Rank
	Acc+	NQA	Avg	Acc+	NQA	Avg					
Open source MLLMs											
VisualGLM [20]	3.46	1.83	3.13	4.22	4.84	4.35	3.68	#18	18.96	6.80	12.88
Shikra [13]	8.59	2.35	7.34	7.50	9.05	7.81	7.55	#17	16.24	7.28	11.76
OneChart [10]	12.34	2.26	10.33	8.75	3.37	7.68	9.12	#16	85.30	49.10	67.20
InstructBLIP [17]	17.96	0.87	14.55	5.50	5.37	5.47	10.43	#15	15.92	7.92	11.92
ChartVLM [74]	8.02	43.74	15.24	5.92	18.21	8.37	12.06	#14	42.08	82.48	62.28
InternLM-XComposer [82]	19.70	1.22	16.01	10.11	5.79	9.25	12.94	#13	13.20	7.84	10.52
CogVLM-Chat [70]	14.41	12.96	14.12	11.89	13.68	12.25	13.26	#12	34.24	28.56	31.40
SPHINX [41]	17.87	6.17	15.54	17.92	12.74	16.89	16.13	#11	21.44	11.20	16.32
BLIP2 [38]	21.65	0.96	17.53	18.44	4.84	15.74	16.70	#10	13.52	6.00	9.76
CogAgent [27]	20.39	26.61	21.63	14.36	25.79	16.64	19.35	#9	54.08	80.56	67.32
MiniGPT-v2 [12]	22.37	2.43	18.40	25.06	5.26	21.11	19.61	#8	15.60	8.48	12.04
ChartLlama [26]	22.02	16.87	21.00	22.56	18.32	21.71	21.30	#7	58.40	93.12	75.76
mPLUG-Owl-bloomz [78]	27.80	2.35	22.73	25.47	6.21	21.64	22.21	#6	7.84	4.88	6.36
LLaVA-v1.5 [46]	25.61	8.09	22.12	27.39	15.26	24.97	23.39	#5	22.64	13.04	17.84
Qwen-VL-Chat [4]	29.46	23.57	28.28	26.56	21.05	25.46	26.98	#4	42.48	75.20	58.84
DocOwl-v1.5 [29]	35.27	37.30	35.67	26.86	29.47	27.38	31.89	#3	48.24	86.72	67.48
Mini-Gemini [40]	39.57	25.57	36.78	31.81	25.79	30.61	33.96	#2	44.32	57.04	50.68
InternLM-XComposer-v2 [19]	57.89	40.96	54.52	41.75	31.58	39.73	47.78	#1	63.12	81.92	72.64
Closed source MLLMs											
ERNIE [5]	47.39	25.74	43.08	46.39	33.37	43.82	43.37	#3	-	-	-
GPT-4V [54]	53.26	33.04	49.23	55.83	40.00	52.68	50.74	#2	-	-	78.50
GPT-4O [54]	65.00	40.00	60.02	63.33	41.05	58.89	59.45	#1	-	-	85.70

- A. Light green.
- B. Yellow.
- C. Orange.
- D. Light blue.
- E. Purple..

Ground Truth: B. Yellow.

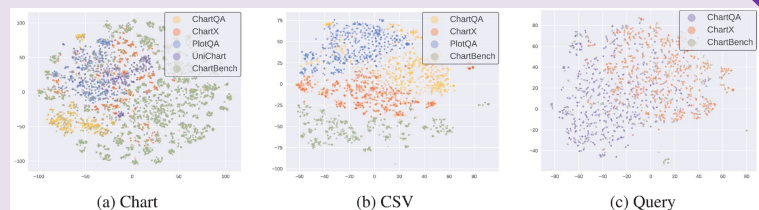
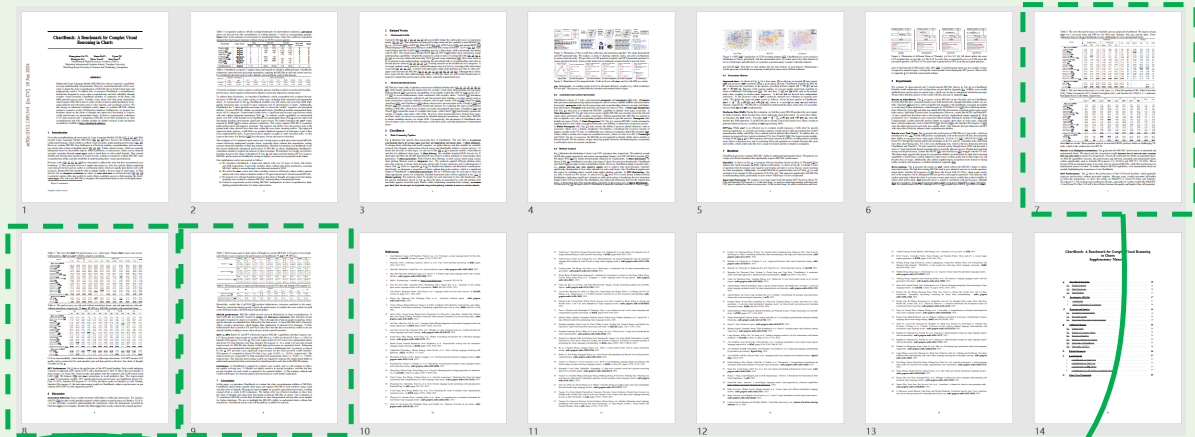


Figure S.14. The demo of figure-table comprehension.

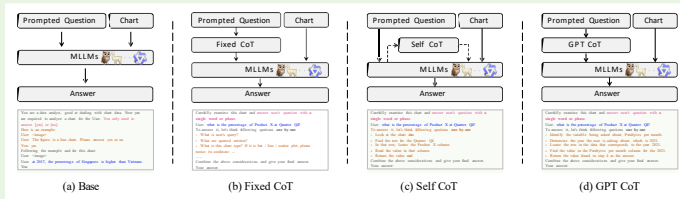
Figure-Text Comprehension

Document Thumbnail:



Question: Based on the analysis presented in the corresponding paragraph, which combination in the illustration of different chain of thought examples, demonstrates the highest and lowest performance, respectively?

Evidence:



CoT Performance. Tab. 7 shows the performance of the CoT-based baseline, which generally improves performance without parameter updates. Because many models encounter difficulties in following instructions, we show the results on MiniGPT-v2, Qwen-VL-Chat, and Internlm-XComposer-v2. The fixed prompt ameliorates all tasks, especially for weaker models like MiniGPT-v2 and Qwen-VL-Chat. CoT-self is less effective because the quality and length of the self-generated CoT are uncontrollable, which hinders models from following instructions. CoT-GPT ensures CoT quality and is customized for each question type and thus performs the best. See chain of thought examples in Fig. 4.

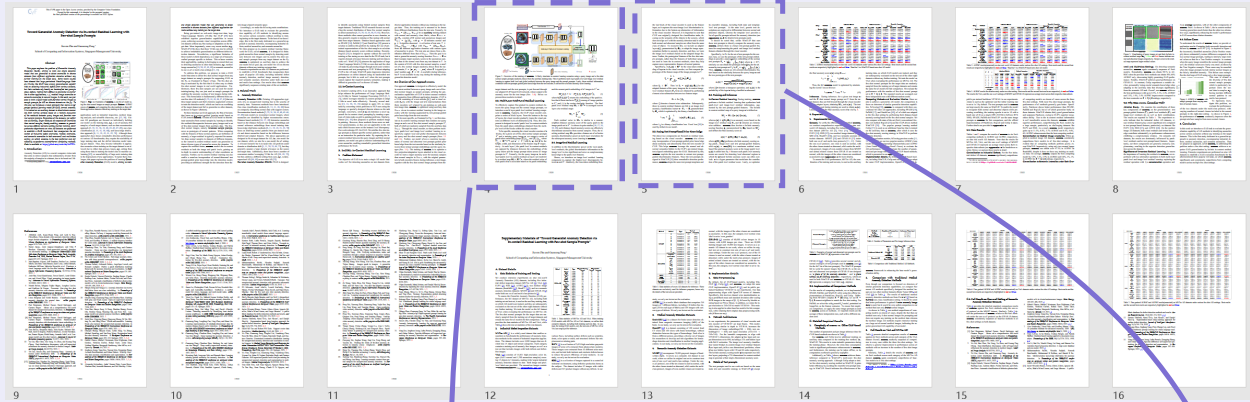
- A. The second one from the left and the third one from the left.
- B. The second one from the left and the rightmost one.
- C. The third one from the left and the rightmost one.
- D. The rightmost one and the third one from the left.
- E. The rightmost one and the second one from the left.

Ground Truth: D. The rightmost one and the third one from the left.

Figure S.15. The demo of figure-text comprehension.

Figure-Formula Comprehension

Document Thumbnail:

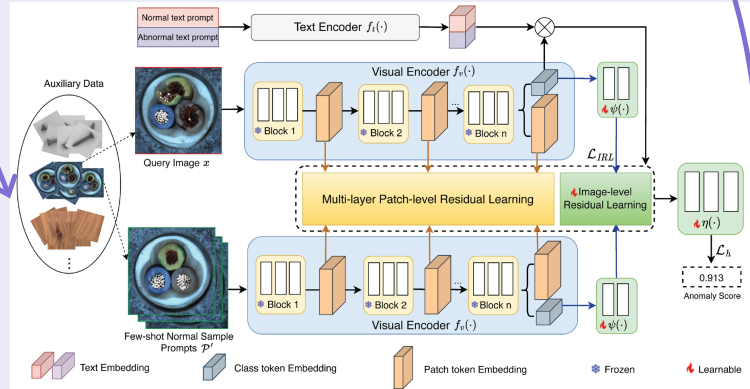


Question: Which colored rectangular volume in the InCTRL architecture are utilized to compute $s_a(x)$ (i.e. the probability of the input x being classified as abnormal)?

- A. Green and light orange.
- B. Pale blue and light orange.
- C. Light orange and yellow.
- D. Pale blue and green.
- E. Pale red and light purple.

Ground Truth: E. Pale red and light purple.

Evidence:

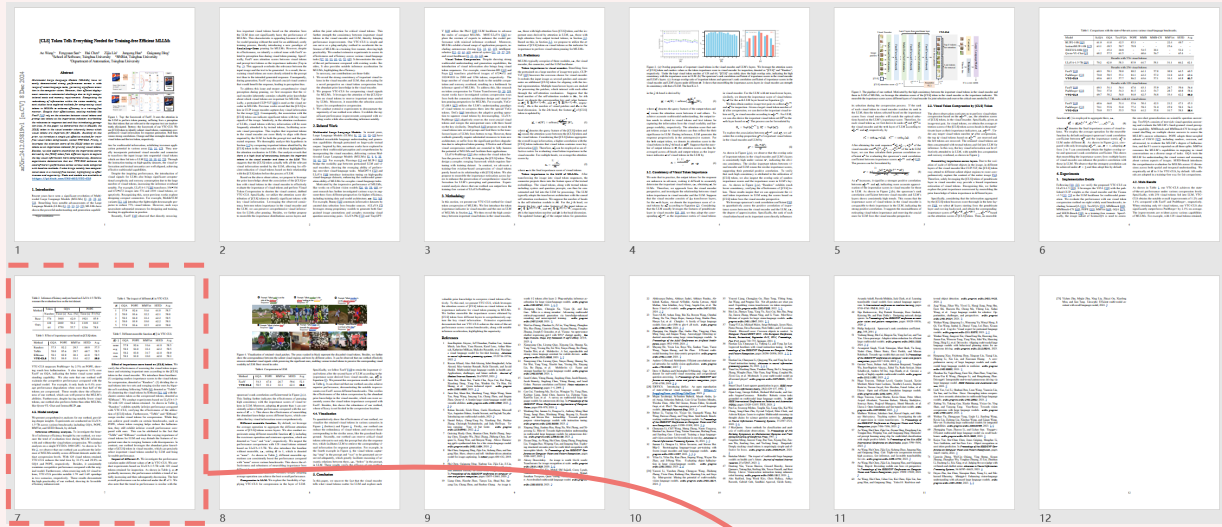


$$s_a(x) = \frac{\exp(F_a^T f_v(x))}{\exp(F_n^T f_v(x)) + \exp(F_a^T f_v(x))}$$

Figure S.16. The demo of figure-formula comprehension.

Table Comprehension

Document Thumbnail:



Question: Among the various ensemble functions adapted in the VTC-CLS method, which one exhibits the best performance on the GQA benchmark?

Evidence:

- A. "Median."
- B. "Max."
- C. "Min."
- D. "None."
- E. "Avg."

Table 5. Different ensemble function $E(\cdot)$ in VTC-CLS.

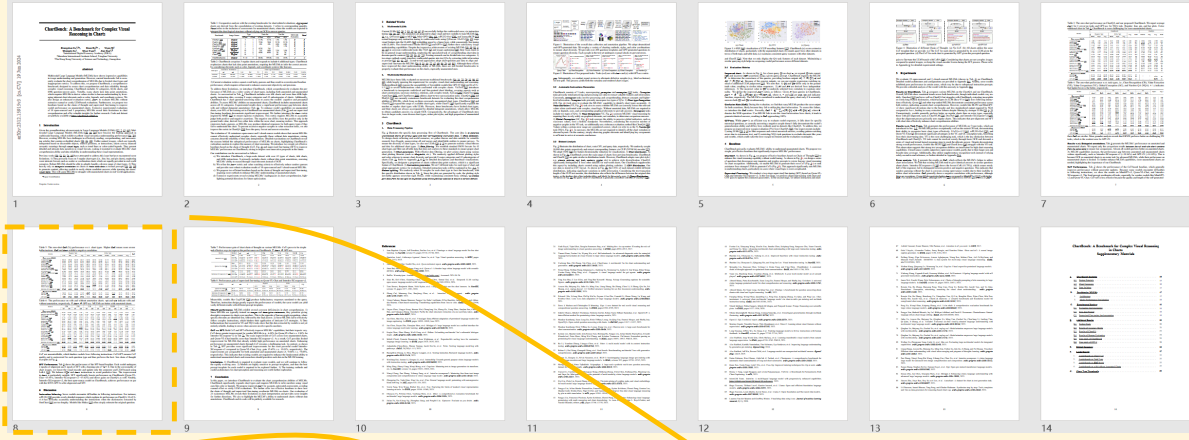
$E(\cdot)$	GQA	POPE	MMVet	SEED	Avg
none	57.9	82.6	31.6	61.8	58.5
avg	58.2	84.0	33.4	62.2	59.5
max	58.2	83.8	31.7	61.8	58.9
min	58.3	83.8	33.0	62.0	59.3

Ground Truth: C. "Min."

Figure S.17. The demo of table comprehension.

Multi-table Comprehension

Document Thumbnail:



Question: In Table 3, what is the average score rank on ChartBench for the open-source MLLM which demonstrates the lowest NQA score among its peers in Table 4?

- A. #18.
- B. #16.
- C. #10.
- D. #12.
- E. #17.

Evidence:

Table 3: The zero-shot performance on ChartQA and our proposed ChartBench. We report average $Acc+$ for 4 yes-or-no tasks and GPT-acc for NQA task. Regular: line, pie, and bar plots. Extra: additional chart in Tab. 2. ChartBench is more challenging for more unannotated charts.

Models	ChartBench						ChartQA					
	Regular Type			Extra Type			Avg	Rank	Human	Avg	Rank	
	Acc+	NQA	Avg	Acc+	NQA	Avg						
Open source MLLMs												
VisualGLM [20]	3.46	1.83	3.13	4.22	4.84	4.35	3.68	#18	18.96	6.80	12.88	#12
Shiken [13]	8.59	2.35	7.34	7.50	9.05	7.81	7.55	#17	16.24	7.28	11.76	#15
OneChart [10]	12.34	2.26	10.33	8.75	3.37	7.68	9.12	#16	85.30	49.10	67.20	#5
InstructBLIP [17]	17.96	0.87	14.55	5.50	5.37	5.47	10.43	#15	15.92	7.92	11.92	#14
ChartVLM [74]	8.02	43.74	15.24	5.92	18.21	8.37	12.06	#14	42.08	82.48	62.28	#6
InternLM-Xcomposer [82]	19.70	1.22	16.01	10.11	5.79	9.25	12.94	#13	13.20	7.84	10.52	#16
CogVLM-Chat [70]	14.41	12.96	14.12	11.89	13.68	12.25	13.26	#12	34.24	28.56	31.40	#9
SPHINX [41]	17.87	6.17	15.54	17.92	12.74	16.89	16.13	#11	21.44	11.20	16.32	#11
BLIP2 [38]	21.65	0.96	17.53	18.44	4.84	15.74	16.70	#10	13.52	6.00	9.76	#17
CogAgent [27]	20.39	26.61	21.63	14.36	25.79	16.64	19.35	#9	54.08	80.56	67.32	#4
MiniGPT-v2 [12]	22.37	2.43	18.40	25.06	5.26	21.11	19.61	#8	15.60	8.48	12.04	#13
ChartLlama [26]	22.02	16.87	21.00	22.56	18.32	21.71	21.30	#7	58.40	93.12	75.76	#1
mPLUG-Owl-bloomz [78]	27.80	2.35	22.73	25.47	6.21	21.64	22.21	#6	7.84	4.88	6.36	#18
LLaVA-v1.5 [46]	25.61	8.09	22.12	27.39	15.26	24.97	23.39	#5	22.64	13.04	17.84	#10
Qwen-VL-Chat [4]	29.46	23.57	28.28	26.56	21.05	25.46	26.98	#4	42.48	75.20	58.84	#7
DocOwl-v1.5 [29]	35.27	37.30	35.67	26.86	29.47	27.38	31.89	#3	48.24	86.72	67.48	#3
Mini-Gemini [40]	39.57	25.57	36.78	31.81	25.79	30.61	33.96	#2	44.32	57.04	50.68	#8
InternLM-Xcomposer-v2 [19]	57.89	40.96	54.52	41.75	31.58	39.73	47.78	#1	63.12	81.92	72.64	#2
Closed source MLLMs												
ERNIE [5]	47.39	25.74	43.08	46.39	33.37	43.82	43.37	#3	-	-	-	
GPT-4V [54]	53.26	33.04	49.23	55.83	40.00	52.68	50.74	#2	-	-	78.50	#2
GPT-4O [54]	65.00	40.00	60.02	63.33	41.05	58.89	59.45	#1	-	-	85.70	#1

Table 4: The zero-shot performance w.r.t. task types, i.e., Chart Recognition (CR), Value Extraction (VE), Value Comparison (VC), Global Conception (GC), and Number QA (NQA). \uparrow / \downarrow indicates that higher/lower is the better, respectively.

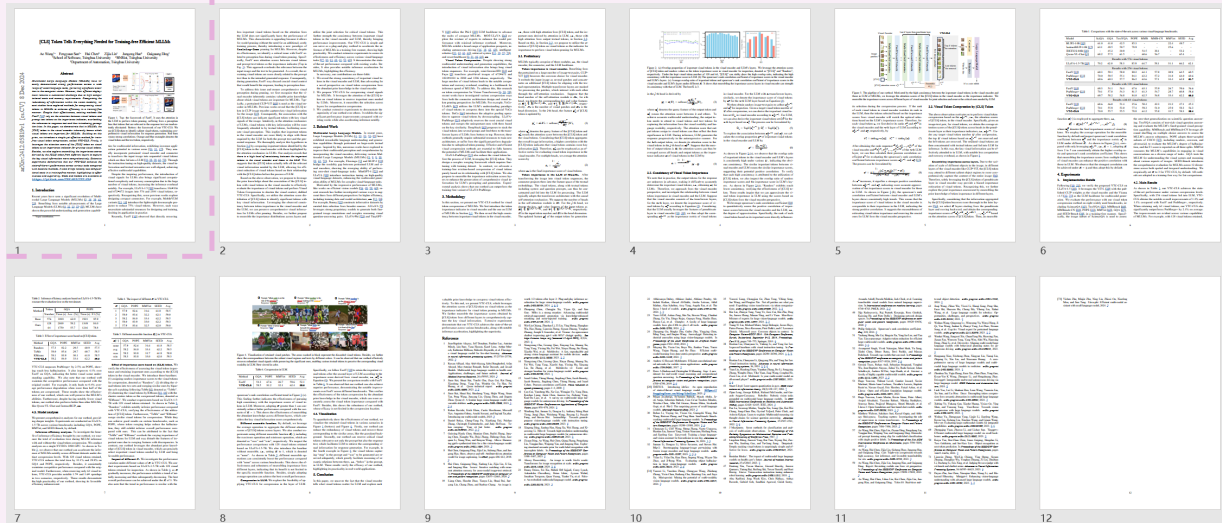
Models	CR		VE		VC		GC		NQA \uparrow	Avg. \uparrow
	Acc \uparrow	CoR \downarrow	Acc \uparrow	CoR \downarrow	Acc \uparrow	CoR \downarrow	Acc \uparrow	CoR \downarrow		
Open source MLLMs										
VisualGLM [20]	16.29	79.19	0.00	99.67	0.00	99.81	0.00	99.71	3.19	3.68
Shiken [13]	2.10	93.57	11.90	80.71	10.62	87.71	7.86	93.71	5.38	7.55
OneChart [10]	3.71	94.33	15.48	82.14	17.57	73.71	11.38	85.67	2.36	9.12
InstructBLIP [17]	49.57	36.67	0.00	100.00	0.05	99.81	0.00	99.90	2.90	10.43
ChartVLM [74]	0.00	100.00	9.05	85.48	10.05	83.81	8.52	86.19	32.19	12.06
InternLM-Xcomposer [82]	42.29	56.95	6.86	85.14	2.48	96.57	9.67	78.48	3.29	12.94
CogVLM [70]	29.14	69.33	2.81	94.29	14.19	80.71	7.33	90.14	13.29	13.26
SPHINX [41]	38.48	51.38	10.38	80.67	14.33	77.38	9.62	80.90	9.14	16.13
BLIP2 [38]	60.05	37.05	4.24	89.29	14.05	78.86	3.86	90.00	2.71	16.70
MiniGPT-v2 [12]	29.05	49.24	22.00	55.14	24.29	53.33	18.10	61.76	3.71	19.35
CogAgent [27]	62.57	37.10	1.19	94.90	7.33	88.24	1.19	94.76	26.24	19.61
ChartLlama [26]	49.86	44.19	8.38	84.14	20.43	69.48	10.67	83.81	17.52	21.30
mPLUG-Owl-bloomz [78]	32.33	51.24	23.14	76.76	25.33	69.29	26.48	71.00	4.00	22.21
LLaVA-v1.5 [46]	47.86	36.24	15.81	66.24	26.05	56.48	16.52	66.57	11.33	23.39
Qwen-VL-Chat [4]	51.67	42.71	11.14	84.57	27.29	63.14	21.71	74.86	22.43	26.98
DocOwl-v1.5 [29]	30.43	65.05	34.48	58.24	31.10	55.19	30.48	63.19	33.76	31.89
Mini-Gemini [40]	80.52	17.86	17.62	70.43	26.00	59.38	22.00	71.10	25.67	33.96
InternLM-Xcomposer-v2 [19]	68.29	30.24	36.63	57.71	54.63	27.71	45.80	51.46	36.71	47.78
Closed source MLLMs										
ERNIE [5]	65.24	19.52	44.76	44.76	32.86	41.43	47.14	47.62	29.24	43.37
GPT-4V [54]	96.19	2.86	30.95	63.33	48.57	34.76	46.19	47.62	36.19	50.74
GPT-4O [54]	97.62	1.43	43.33	44.76	66.19	16.19	53.33	41.43	40.48	59.45

Ground Truth: C. #10.

Figure S.18. The demo of multi-table comprehension.

Text Comprehension

Document Thumbnail:



Evidence:

Despite the inspiring performance, the introduction of visual signals for LLMs also brings significant computational complexity and memory consumption due to the large number of visual tokens, increasing the inference overhead notably. For example, LLaVA-1.5 [38] transforms 336×336 and 672×672 images into 576 and 2304 visual tokens, respectively. Recognizing this, some previous works explore designing compact connectors. For example, MobileVLM variants [13, 14] introduce the lightweight downsample projector to reduce 75% visual tokens. However, such ways necessitate substantial resources for designing and training, limiting its application in practice.

Question: Based on the discussion in the paper, which of the following accurately represents the limitations of MobileVLM variants?

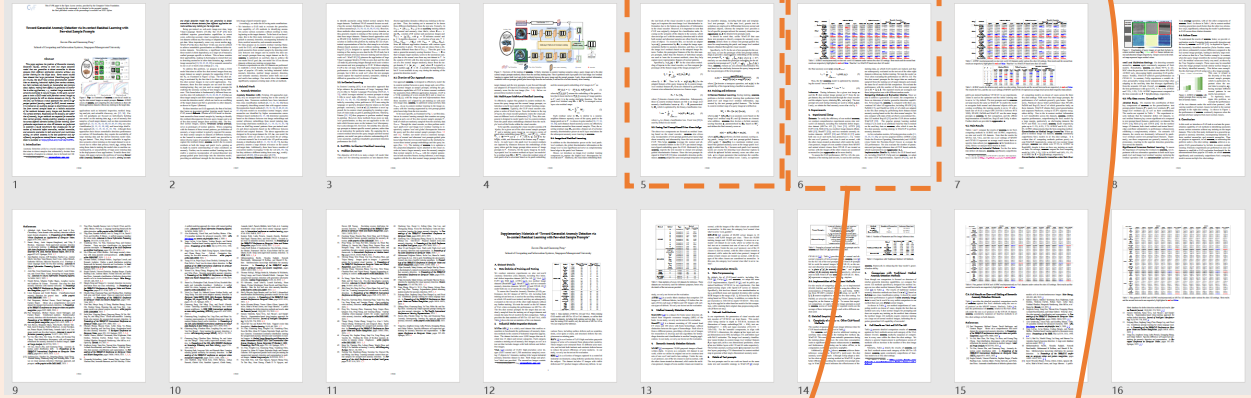
- A. Requiring substantial resources for designing and training.
- B. Directly removing less important visual tokens based on the attention from the LLM.
- C. Overlooking the relevance between the input image and the text to be generated.
- D. Discarding crucial visual context that would benefit the response.
- E. Demonstrating limited adaptability to diverse visual input formats and resolutions.

Ground Truth: A. Requiring substantial resources for designing and training.

Figure S.19. The demo of text comprehension.

Formula Comprehension

Document Thumbnail:



Question: In the inference process, which numbered equation describes how the final anomaly score is computed for a given test image x_t ?

Evidence:

the final anomaly score $s(x)$ using X_{train} :

$$\mathcal{L}_h = \frac{1}{N} \sum_{x \in X_{tr}} \mathcal{L}_b(s(x), y_x). \quad (9)$$

Thus, the full InCTRL model is optimized by minimizing the overall loss as follows:

$$\mathcal{L}_{InCTRL} = \mathcal{L}_{IRL} + \mathcal{L}_h. \quad (10)$$

Inference. During inference, for a given test image x_t and the K -shot normal image prompt set \mathcal{P} from the target dataset, they are fed forward through the visual encoder and the adapter layers, obtaining \mathbf{M}_{x_t} and $s_i(x_t)$. The text prompt sets used during training are used to obtain $s_a(x_t)$. Lastly, we obtain the final anomaly score of x_t via Eq. 8.

$$s_a(x) = \frac{\exp(\mathbf{F}_d^T f_v(x))}{\exp(\mathbf{F}_d^T f_v(x)) + \exp(\mathbf{F}_d^T f_v(x))}, \quad (6)$$

where $[\cdot]^T$ denotes a transpose operation, and $s_a(x)$ is the probability of the input x being classified as abnormal.

3.6. Training and Inference

In-Context Residual Learning. During training, InCTRL performs a holistic residual learning that synthesizes both patch-level and image-level residual information, augmented by the text prompt-guided features. The holistic in-context residual map of a query image x is defined as:

$$\mathbf{M}_x^+ = \mathbf{M}_x \oplus s_i(x) \oplus s_a(x), \quad (7)$$

where $s_i(x) = \eta(\mathbf{F}_x; \Theta_\eta)$ is an anomaly score based on the image-level residual map \mathbf{F}_x and \oplus denotes an element-wise addition. InCTRL then devises a holistic anomaly scoring function ϕ , parameterized by Θ_ϕ , based on \mathbf{M}_x^+ , and defines the final anomaly score as:

$$s(x) = \phi(\mathbf{M}_x^+; \Theta_\phi) + \alpha s_p(x), \quad (8)$$

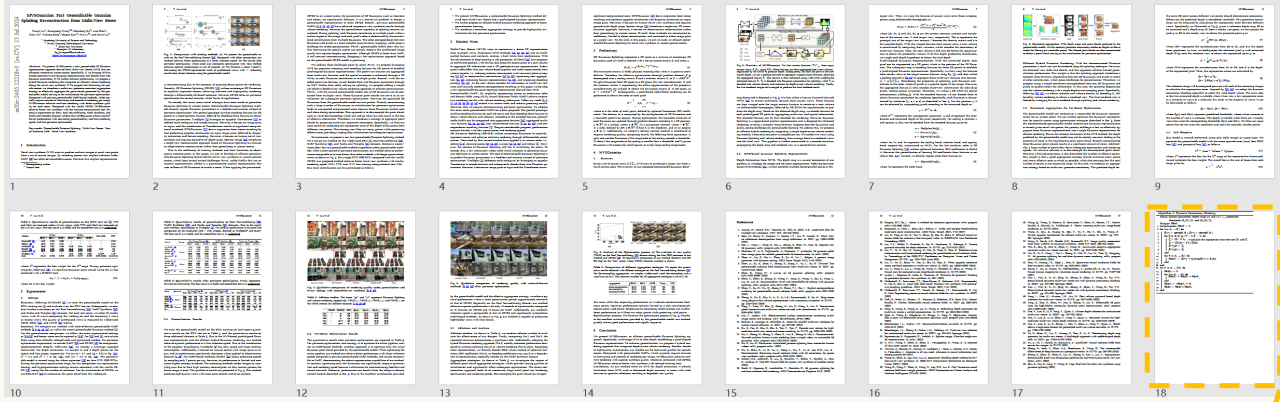
- A. Equation (10).
- B. Equation (9).
- C. Equation (8).
- D. Equation (7).
- E. Equation (6).

Ground Truth: C. Equation (8).

Figure S.20. The demo of formula comprehension.

Pseudocode Comprehension

Document Thumbnail:



Question: How many steps are there in the Dynamic Consistency Checking algorithm?

- A. 21.
- B. 18.
- C. 24.
- D. 16.
- E. 20.

Ground Truth: A. 21.

Evidence:

Algorithm 1: Dynamic Consistency Checking

Input: Camera parameters, Depth maps D_0 and $\{D_i\}_{i=1}^N$, predefined thresholds $\{\theta_p(n)\}_{n=1}^{N_\theta}$ and $\{\theta_d(n)\}_{n=1}^{N_\theta}$

Output: $Mask$

```

1 Initialization:  $Mask \leftarrow 0$ 
2 for  $i$  in  $(1, \dots, N)$  do
3    $Err_p^i \leftarrow zeros(H, W)$ ,  $Err_d^i \leftarrow zeros(H, W)$ 
4   for  $p$  in  $(0, 0)$  to  $(H-1, W-1)$  do
5      $\xi_p^i \leftarrow \|p - p'\|_2$ ,  $\triangleright$  calculate the reprojection error between  $D_0$  and  $D_i$ 
6      $\xi_d^i \leftarrow \|D_0(p) - d'\|_1 / D_0(p)$ 
7      $Err_p^i(p) \leftarrow \xi_p^i$ 
8      $Err_d^i(p) \leftarrow \xi_d^i$ 
9   end
10  for  $n$  in  $(1, \dots, N_\theta)$  do
11     $Mask_n^i \leftarrow (Err_p^i < \theta_p(n)) \& (Err_d^i < \theta_d(n))$ 
12  end
13 end
14 for  $n$  in  $(1, \dots, N_\theta)$  do
15    $Mask_n \leftarrow 0$ 
16   for  $i$  in  $(1, \dots, N)$  do
17      $Mask_n \leftarrow Mask_n + Mask_n^i$ 
18   end
19    $Mask_n \leftarrow (Mask_n > n)$ 
20    $Mask \leftarrow Mask \cup Mask_n$ 
21 end

```

Figure S.21. The demo of pseudocode comprehension.

I. Hallucinated Evidence: Case

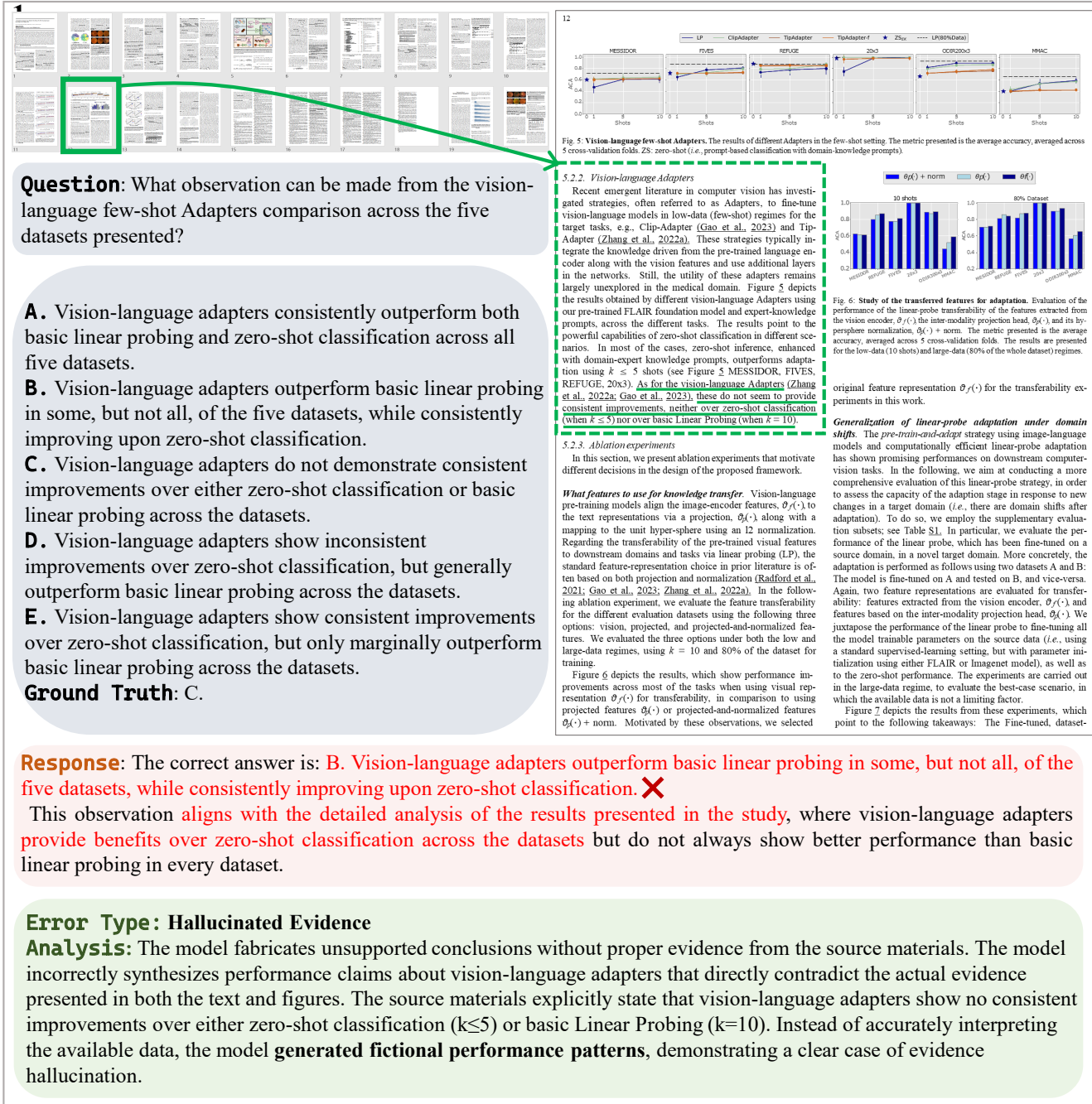


Figure S.22. Illustration of a Hallucinated Evidence Error Case. The figure demonstrates how the model fabricates unsupported conclusions about vision-language adapter performance, contradicting the evidence highlighted in green from the source materials.

Question: What observation can be made from the vision-language few-shot Adapters comparison across the five datasets presented?

A. 2; 36 hours..
 B. 3; 40 hours..
 C. 2; 40 hours..
 D. 3; 36 hours..
 E. 3; 45 hours

Ground Truth: C.

Response: The correct answer is: A. 2; 36 hours. ❌

Error Type: Incomplete Evidence

Analysis: The model's response demonstrates **selective attention to the available evidence**. While accurately identifying the two-stage nature of the visual pre-training process from the text "The visual pre-training process involves two stages," in the paper, it **only captured partial evidence information for the second question**. Specifically, the model focused on "the second stage took around 36 hours" while **overlooking the crucial detail that "the first stage took approximately 4 hours."** A complete consideration of both time components would yield a total of 40 hours (4 + 36), making C the correct answer. This partial evidence consideration led to an inaccurate conclusion.

Published as a conference paper at A4MAT-Vienna 2024

Table 11: Hyperparameters for visual language pre-training on interleaved text and image data.

Hyperparameter	Values
base model	https://huggingface.co/meta-llama/llama-2-7b-hf
vision encoder	https://huggingface.co/openai/clip-vit-large-patch14-336
projector	2-layer MLP
Stage 1: Projector Initialization	
epochs	1
global batch size	256
learning rate	0.001
learning rate scheduler	cosine
weight decay	0.0
warmup ratio	0.03
max length	4096
tune LLM	✗
tune vision encoder	✓
tune projector	✓
Stage 2: Visual Language Pre-training	
epochs	1
global batch size	128
learning rate	0.0005
learning rate scheduler	cosine
weight decay	0.0
warmup ratio	0.03
max length	4096
tune LLM	✓
tune vision encoder	✗
tune projector	✓

Training Stages The visual pre-training process (Lin et al., 2023) involves two stages:

- 1. Projection initialization:** In this stage, the LLM and the visual encoder are both pre-trained and remain fixed. The projector, however, is randomly initialized. Only the projector is fine-tuned during this stage, using image-caption pairs from (Liu et al., 2024).
- 2. Visual language pre-training:** During this stage, both the LLM and the projector are fine-tuned on the interleaved image and text data. This includes data from general domains provided by MMC4 (Zhu et al., 2024), as well as scientific articles and figures from our dataset MMS-c1. Previous research (Lin et al., 2023) has shown that tuning both the LLM and the projector yields better results than tuning only one of them. Throughout this stage, the visual encoder remains fixed.

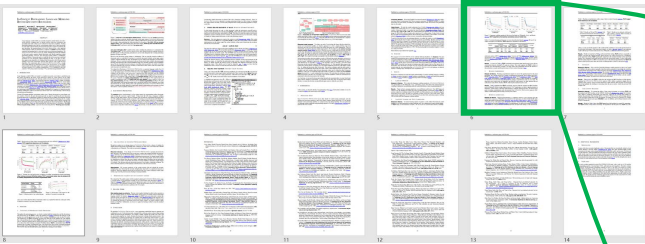
We did not conduct the further visual instruction-tuning for this model, as our primary objective was to infuse scientific knowledge into the LLM for the consecutive text-only material generation task. The two stages were conducted on a computing cluster equipped with eight NVIDIA A100 GPUs, each with 40GB of memory. **The first stage took approximately 4 hours, and the second stage took around 36 hours.**

A.3.5 MATERIALS GENERATION

As a case study to investigate whether scientific knowledge has been effectively infused into the LLM (LLaMA2-7B in our experiments) and whether it can enhance performance on material science-related tasks, we follow the methodology from Gruver et al. (2024) to explore the material generation task. The primary objective is to format material crystal structures into text strings and fine-tuning the LLM to generate stable materials.

Prompt design We adhere to the prompt design described in (Gruver et al., 2024). There are two types of prompts in the training data: the generation prompt with one or multiple conditions and infilling prompts, where partial crystal structure strings are masked and the model generates the masked parts. The specific prompt templates are shown below, adapted from (Gruver et al., 2024).

III. Perceptual Error: Case 1



Question: Referring to the color scheme in Figure 3's legend, what are the respective Sentiment-Amazon scores in Table 1 for the methods represented by blue, green and pink?

- A. 80.2, 83.7, 93.2.
 - B. 94.6, 88.0, 96.5.
 - C. 61.8, 66.0, 71.3.
 - D. 88.0, 94.6, 96.5.
 - E. 96.5, 94.6, 88.0.
- Ground Truth:** D.

Response: To answer this question, we align the methods represented by their respective colors in Figure 3's legend with the Sentiment-Amazon scores in Table 1. From Figure 3:

- Blue: Standard method
- Green: kNN method
- Pink: ICLM method

From Table 1 (Sentiment-Amazon column):

- Standard method = 94.6
- kNN method = 88.0
- ICLM method = 96.5

Thus, the respective scores for blue, green, and pink are ****94.6, 88.0, and 96.5****.

The correct answer is: **B. 94.6, 88.0, 96.5. ❌**

Error Type: Perceptual Error

Analysis: This response demonstrates a critical perceptual error in color-method association. While the model correctly identified the numerical scores from Table 1 for each method, it **incorrectly mapped the colors to their corresponding methods in Figure 3's legend**. Specifically, it **reversed the color assignments for the Standard method (actually shown in green, not blue) and the KNN method (actually shown in blue, not green)**. This error highlights a fundamental limitation of current LVLMs in visual-textual alignment tasks, particularly in color-coding interpretation.

Published as a conference paper at ICLR 2024

Figure 3: Language modeling perplexity (the lower the better) on Wikipedia, Arxiv, and Books (§3.3.1). ICLM outperforms the baselines consistently across all model sizes.

Table 1: In-context learning performance on seven classification datasets (§3.3.2). We use 32 in-context examples for all datasets. ICLM outperforms baselines on all datasets.

Method	Sentiment			Hate Speech		Topic Classification		Average
	Amazon	SST2	Yelp	Hate	Offensive	Agnews	Dbpedia	
Standard	94.6	83.7	74.3	52.7	55.7	68.3	61.5	66.0
kNN	88.0	80.2	65.1	50.1	53.1	65.7	56.4	61.8
ICLM	96.5	93.2	77.4	60.6	57.3	76.0	63.2	71.3

Sentiment analysis (SST-2) (Socher et al., 2013), Amazon and Yelp (Zhang et al., 2015a), topic classification (AGN (Zhang et al., 2015b) and Dbpedia (Lehmann et al., 2015)) and hate speech detection (Barbieri et al., 2020). We use label words from Min et al. (2022) and report accuracy as the metric.

Results. As shown in Table 1, ICLM consistently demonstrates better performance across all text classification datasets, leading to 8% gain on average. This result suggests that ICLM is better at learning from demonstration examples. We later analyze the relationship between the number of demonstration examples and the performance of the in-context learning in §4.3.

3. READING COMPREHENSION

Datasets & Metrics. Reading comprehension requires to answer the question based on the given paragraph. We consider the RACE reading comprehension benchmark (RACE-High and RACE-Middle) (Lai et al., 2017), SQuAD (Rajpurkar et al., 2016), BoolQ (Clark et al., 2019), DROP (Dua et al., 2019), and HotpotQA (Yang et al., 2018). We use 2-shot in-context learning for evaluation; we did not use more because some documents in reading comprehension tasks are very long. We report the exact match score for HotpotQA and SQuAD, and accuracy for other datasets that are multi-choice tasks (RACE, BoolQ, DROP), following the standard in prior work.

Results. Table 2 highlights that ICLM consistently surpasses both the standard and kNN baselines across all datasets with an average improvement of 14%. In particular, we observe significant gains on HotpotQA, which requires multi-hop understanding of multiple related documents. The performance gain on reading comprehension tasks demonstrates that In-CONTEXT PRETRAINING improves LMs' ability of understanding and reasoning over the given context.

4. RETRIEVAL-AUGMENTATION

Datasets & Metrics. Retrieval-augmentation is a method to retrieve a set of passages from the external text corpus (e.g., Wikipedia) and prepend it to the input query in order to better handle input queries that require factual knowledge (Lin et al., 2023; Xu et al., 2023; Su et al., 2023). We conduct evaluation on two well-studied open-domain QA datasets: Natural Questions (NQ) (Kwiatkowski et al., 2019) and TriviaQA (Joshi et al., 2017). For both datasets, we report exact match scores (EM) and evaluate the model performance in both closed-book and open-book settings. In the closed-book

6

Figure S.24. Illustration of a Perceptual Error Case. The figure demonstrates how the model correctly identifies numerical scores but incorrectly maps color codes to methods, mismatching the blue and green representations in the legend despite clear visual evidence.

IV. Extractor Error: Case 1

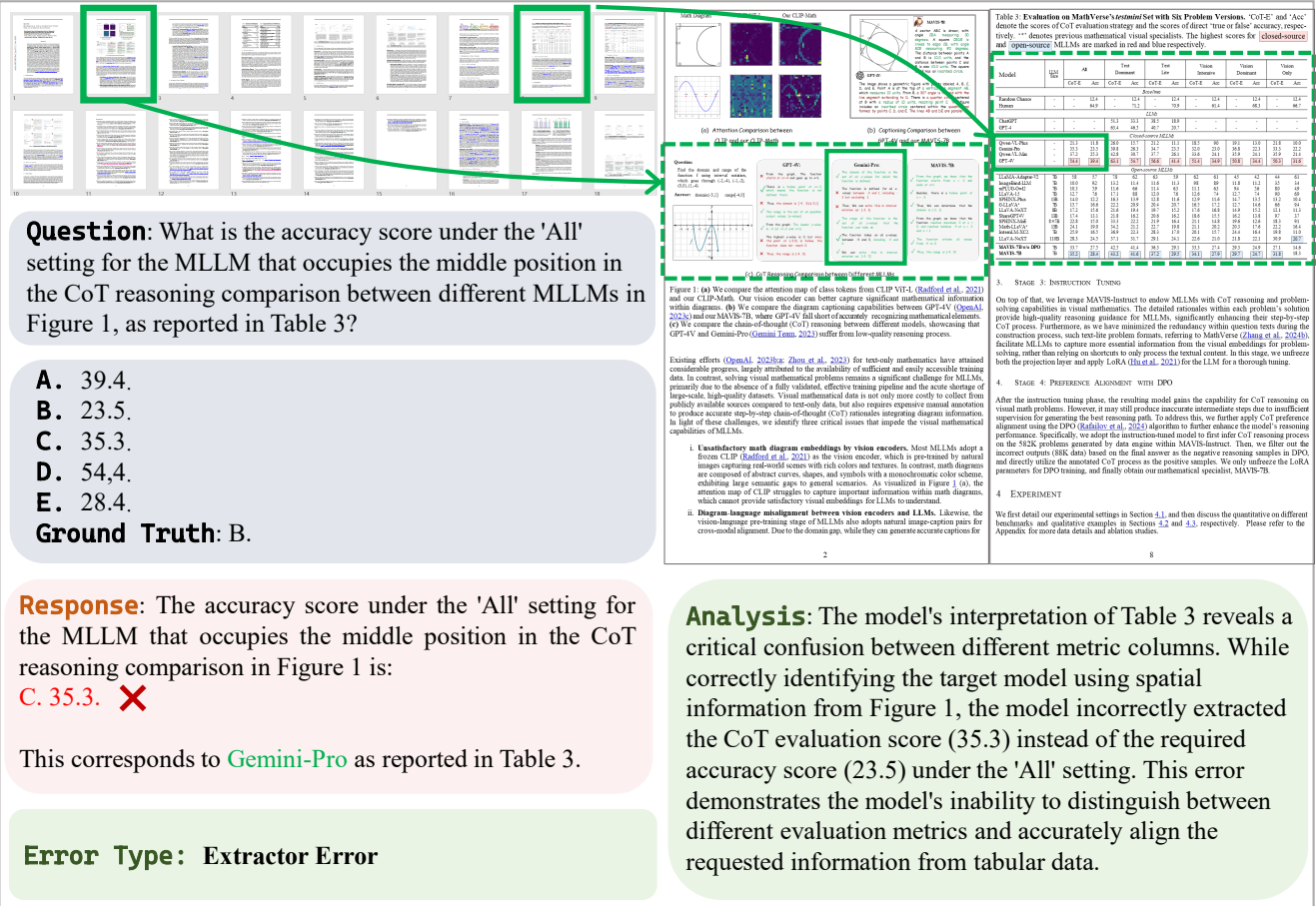


Figure S.25. Illustration of an Extractor Error Case. The figure demonstrates how the model confuses different metric columns in Table 3, extracting the CoT evaluation score (35.3) instead of the correct accuracy score (23.5) despite accurately identifying the target model from spatial information.

V. Reasoning Error: Case 1

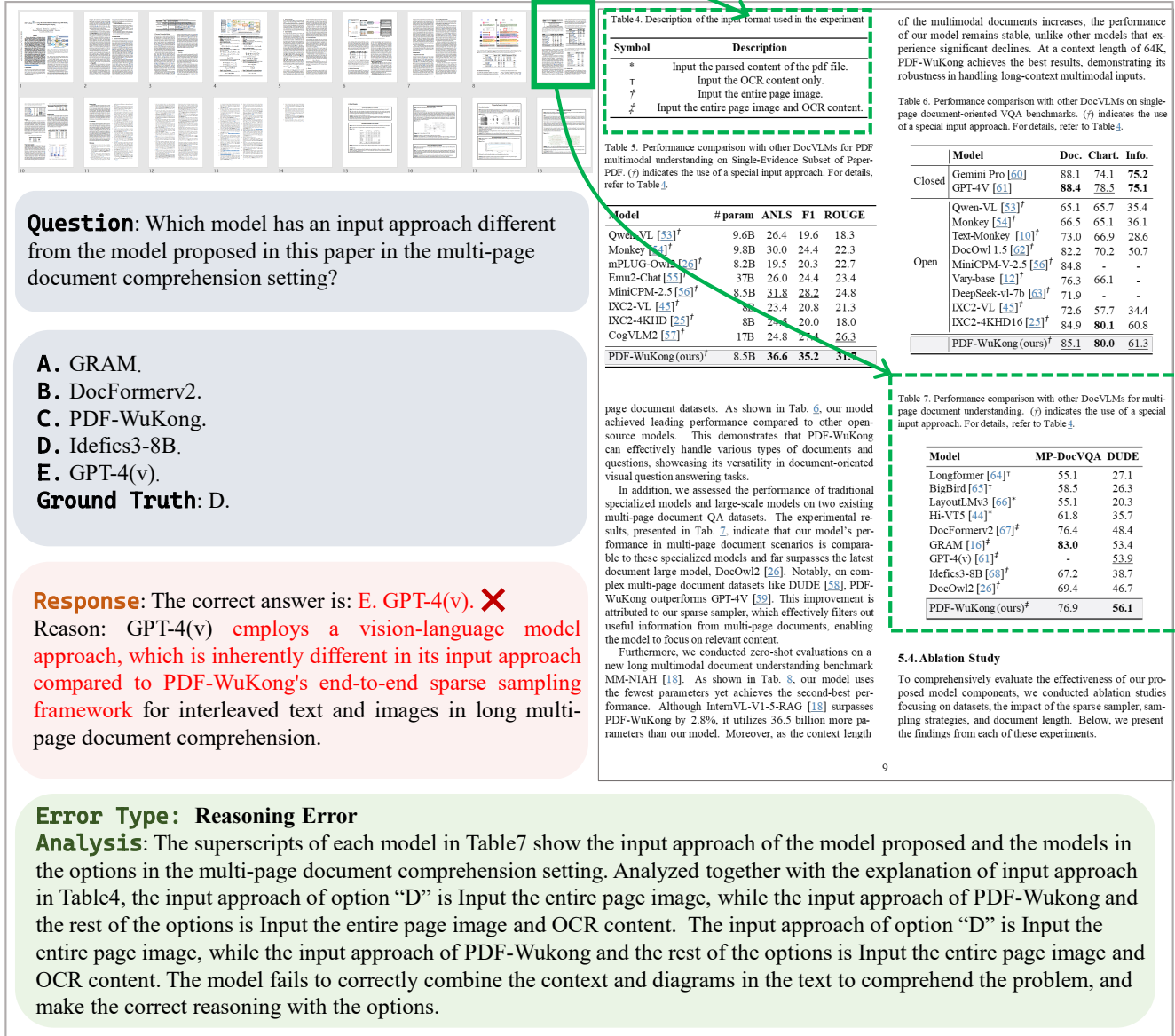


Figure S.26. Illustration of a Reasoning Error Case. The figure demonstrates how the model fails to correctly interpret input approach differences between models despite clear evidence from Table 1 and Table 7, misidentifying GPT-4(v) as having a distinct approach from other models.

VI. Irrelevant Answer: Case 1

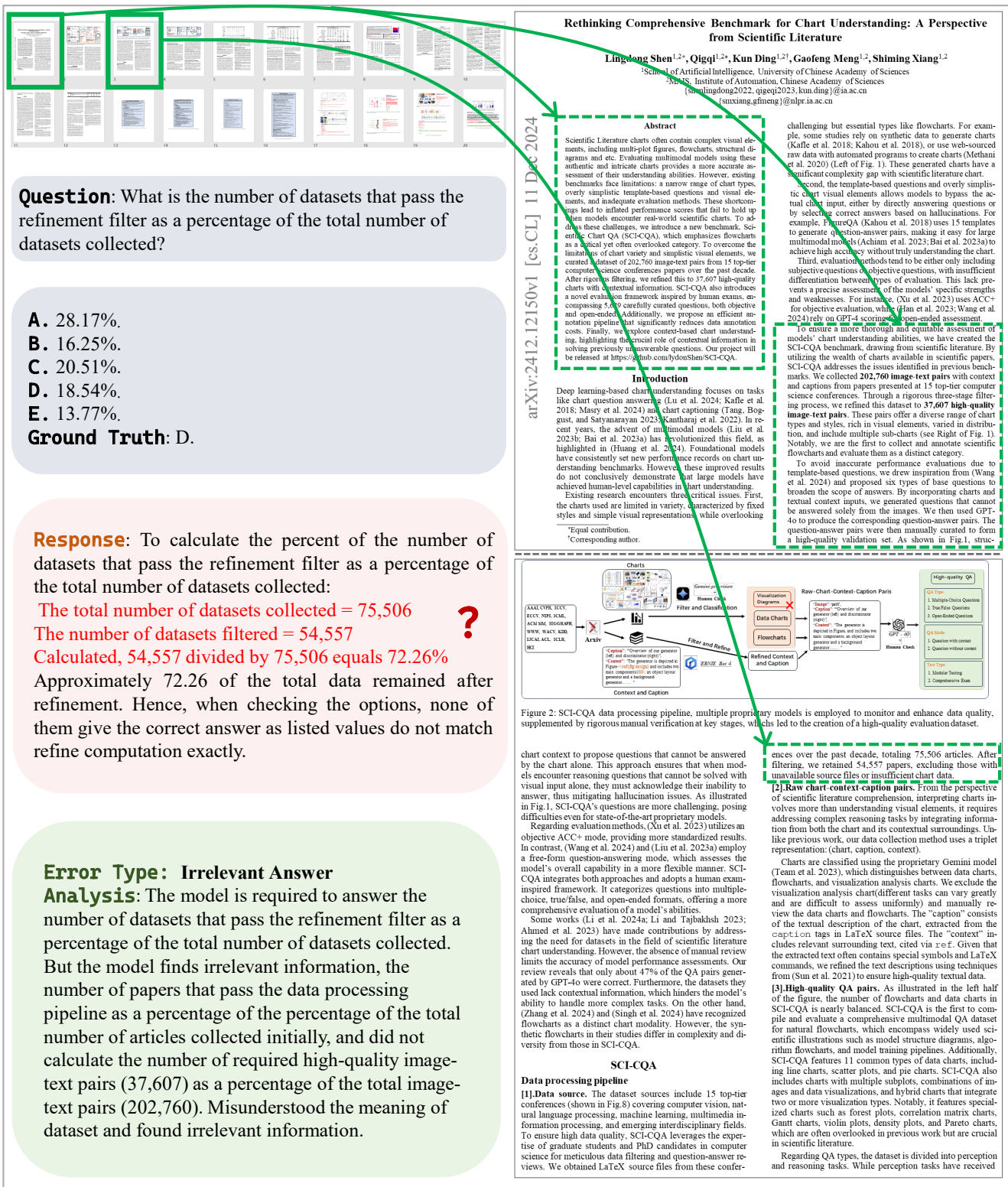
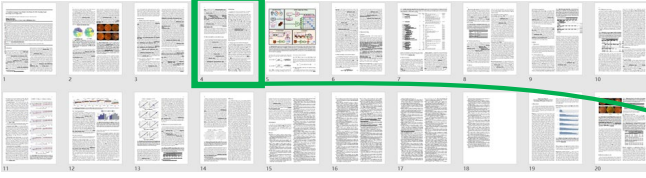


Figure S.27. Illustration of an Irrelevant Answer Case. The figure demonstrates how the model misinterprets the question target, calculating the percentage of papers passing the pipeline (54,557/75,506) instead of the required percentage of high-quality image-text pairs (37,607/202,760), revealing a fundamental misunderstanding of the dataset definition

VII. Matching Error: Case 1



Question: According to the paper, which of the following statements about the text description defined before section '3.1' is True?

A. The text descriptions are designed to provide a one-to-one correspondence between each categorical label and a unique textual representation.

B. A single categorical label may correspond to several text descriptions, each describing a different feature of the image.

C. A single text description may correspond to multiple categorical labels, as various diseases can exhibit similar symptoms..

D. The text descriptions are generated by a Large Language Model that has been fine-tuned on extensive medical imaging data..

E. The text descriptions are annotated by a several invited expert radiologists to ensure accurate representations.

Ground Truth: B.

2023), or attribute descriptions (Menon and Vondrick, 2023) for prompt-based inference, using pre-trained question-answering models to describe the shape and color of the target conditions (Qin et al., 2023). Other works have focused on the pre-training stage, generating domain-specialized VLP models such as ConVirt (Zhang et al., 2022b), PubMedCLIP (Eslami et al., 2022), GLoRIA (Huang et al., 2021b), MedCLIP (Wang et al., 2022c) or MedKlip (Wu et al., 2023), among others (Windsor et al., 2023; Wang et al., 2022a; Müller et al., 2022; Chen et al., 2022b). One of the main challenges of such pre-training lies in the low prevalence of text-based supervision on publicly available datasets. To alleviate this issue, MedCLIP incorporated categorically-labeled samples through label-space alignment (Wang et al., 2022c). Other methods have taken profit from well-established domain tools in radiology such as UMLS and RadGraph to augment the available text reports (Chen et al., 2022b; Wu et al., 2023).

Despite these recent advances in the development of vision-language pre-training strategies in medical imaging, the use of categorically-labeled datasets has been overlooked. In this work, we argue and show that such supervision could still be exploited to train powerful vision-language representations, by encoding expert’s domain knowledge into text supervision.

2.4. Expert knowledge-driven models of fundus images

The idea of integrating domain knowledge into deep learning for medical image analysis is not new, and has triggered interest in the recent literature (Xie et al., 2021). In particular, domain-specific, expert knowledge (EK) from clinicians could be retrieved to highlight areas of interest, relevant features, anatomical priors, or inter-disease dependencies and hierarchies. In retinal imaging, the expert’s knowledge has been integrated in various ways. For instance, Giancardo et al. (2012) first segmented the exudates, which served as a proxy for macular edema detection. Similarly, several other strategies train attention modules to enhance local lesions, which act as surrogates for disease classification. Closely related to our work, we have identified several categories, which include: using pixel-level annotated lesions for AMD staging (Fang et al., 2019), weakly-supervised strategies based on the relationships between diabetic retinopathy and diabetic macular edema (Xiaomeng et al., 2020), or disentangling disease-specific saliency maps for diabetic retinopathy grading (Sun et al., 2021). In addition, expert knowledge for glaucoma detection in fundus images is usually integrated by cropping the optic-disk area as an initial step before classification (Diaz-Pinto et al., 2019; de Vente et al., 2024). Unlike this existing literature, we study the use of well-established expert knowledge on retinal image analysis via vision-language pre-training, which has been largely overlooked in the context of foundation models. Concretely, we propose a contrastive image-text pre-training, which incorporates relevant features, hierarchies, and relationships between the classes as well as information on the regions of interest characterizing the target diseases, in the form of descriptive textual prompts, paired with the corresponding images.

3. Methodology

Fig. 3 depicts an overview of our framework. We introduce each methodological component formally in the following.

Problem setup. Let us define an assembly dataset, \mathcal{D}_T , which contains N samples gathered from different publicly available fundus image datasets, including heterogeneous sources and findings. For each sample, we build a multi-modal triplet including an image, a categorical label and a text description: $\mathcal{D}_T = \{(X_i, y_i, T_i)\}_{i=1}^N$. $X_i \in \mathbb{R}^{D_v}$ denotes a fundus 2D image, with Ω_i its spatial domain, $y_i \in \{1, \dots, C\}$ is a label among the C unique categories in the assembly dataset, and $T_i \in \mathcal{T}$ is a text description associated with the label. Figure 2 provides a few examples of categorical labels, such as DME, and the associated text descriptions encoding domain knowledge, e.g., “hard exudates involving the center of the macula”. Such textual domain knowledge could be derived from the relevant clinical literature (Garner and Ashton, 1979) and/or from community standards (Wilkinson et al., 2003). Table S4 provides a comprehensive list of the correspondences between the categorical labels and textual domain-knowledge descriptions, which we compiled from the relevant clinical literature, to build our foundation model of the retina. Note that a single categorical label may correspond to several text descriptions, each describing a different finding or feature in the image. The objective of our vision-language pre-training is to provide a powerful multi-modal model capable of learning a feature representation space where samples are aligned across the three modalities: images, categories, and text.

3.1. Aligning images, labels and domain-knowledge text

Our multi-modal pre-training integrates vision and language encoders. Let $\Theta = \{\Theta_I(\cdot), \Theta_L(\cdot)\}$ denotes the vision encoder, with $\Theta_I(\cdot)$ a feature extractor and $\Theta_L(\cdot)$ a projection head. The feature extractor $\Theta_I(\cdot)$ yields a feature representation $\mathbf{u} \in \mathbb{R}^{D_u}$: $\mathbf{u} = \Theta_I(X_i)$ of an input image X_i , with D_u the dimension of the visual feature space. Analogously, let $\Phi = \{\Phi_I(\cdot), \Phi_L(\cdot)\}$ denotes the text encoder, $\Phi_I(\cdot)$ being a feature extractor and $\Phi_L(\cdot)$ a projection head. The feature extractor $\Phi_I(\cdot)$ provides an embedding $\mathbf{v} \in \mathbb{R}^{D_v}$: $\mathbf{v}_j = \Phi_I(T_j)$ of an input text T_j , with D_v denoting the dimension of the space of text features. Each of the projection heads, $\Theta_L(\cdot)$ and $\Phi_L(\cdot)$, maps the independent modality representations into a joint unit hyper-sphere space: $\mathbf{u} = \frac{\Theta(\mathbf{u})}{\|\Theta(\mathbf{u})\|}$ and $\mathbf{v} = \frac{\Phi(\mathbf{v})}{\|\Phi(\mathbf{v})\|}$. In this normalized space, the similarity between image X_i and text description T_j is evaluated by the cosine similarity, $\mathbf{u}^T \mathbf{v}$, where T^T denotes the transpose operator.

The objective consists of learning feature representations that minimize the distances between paired image and text descriptions while maximizing the distances between unpaired samples. We build image-text pairs from the available categorical label information, thereby encouraging samples belonging to the same category to have close feature representations, in both the image and text domains. More formally, let \mathcal{B} denote a batch containing a set of images $\{X_i\}_{i \in \mathcal{B}}$ and a set of text descriptions $\{T_j\}_{j \in \mathcal{T}_B}$, where $\mathcal{B} \subset \{1, \dots, N\}$ denotes the set of indices of the images in \mathcal{B} , and $\mathcal{T}_B \subset \{1, \dots, N\}$ the set of indices of the text

Response: The correct answer is: B. A single categorical label may correspond to several text descriptions, each describing a different feature of the image. x?

Explanation: According to the text, the authors define text descriptions that encode domain knowledge for each disease. A single categorical label can correspond to multiple text descriptions, as these descriptions aim to capture various features, hierarchies, and dependencies of the related pathology.

Error Type: Matching Error

Analysis: The model correctly made choice “B”, but due to a matching error in the Rule-based methods, the correct choice was not successfully extracted from the model’s answer, resulting in a matching error.

Figure S.28. Illustration of a Matching Error Case.